



## Water resources pollution associated with risks of heavy metals from Vatukoula Goldmine region, Fiji

Satendra Kumar<sup>a</sup>, Abu Reza Md Towfiqul Islam<sup>b,\*</sup>, H.M. Touhidul Islam<sup>b</sup>, Md Hasanuzzaman<sup>b</sup>, Victor Ongoma<sup>c</sup>, Rahat Khan<sup>d</sup>, Javed Mallick<sup>e,\*\*</sup>

<sup>a</sup> School of Geography, Earth Science and Environment, The University of the South Pacific, Laucala Campus, Private Bag, Suva, Fiji

<sup>b</sup> Department of Disaster Management, Begum Rokeya University, Rangpur, 5400, Bangladesh

<sup>c</sup> International Water Research Institute, Mohammed VI Polytechnic University, Lot 660, Hay Moulay Rachid, Ben Guerir, 43150, Morocco

<sup>d</sup> Institute of Nuclear Science and Technology, Bangladesh Atomic Energy Commission, Savar, Dhaka, 1349, Bangladesh

<sup>e</sup> Department of Civil Engineering, King Khalid University, Abha, Saudi Arabia

### ARTICLE INFO

#### Keywords:

Water and sediment pollution  
Statistical approaches  
Source apportionment  
Environmental and ecological risks assessment  
Health risks appraisal

### ABSTRACT

Although mining is essential for human economic development, is amongst the most polluting anthropogenic sources that influence seriously in water resources. Thus, understanding the presence and concentration of heavy metals in water and sediment in the vicinity of mines is important for the sustainability of the ecosystem. In this work, a multidisciplinary approach was developed to characterize the contamination level, source apportionment, co-existence, and degree of ecological and human health risks of HMs on water resources in the Vatukoula Goldmine region (VGR), Fiji. The outcomes suggested significant contamination by Cd (range: 0.01–0.95 g/L), Pb (range: 0.03–0.53 g/L), and Mn (range: 0.01–3.66 g/L) in water samples surpassed the level set by Fiji and international laws, whereas higher concentration of Cd (range: 2.60–23.16 mg/kg), Pb (range: 28.50–200.90 mg/kg) and Zn (range: 36.50–196.66 mg/kg) were detected in sediment samples. Lead demonstrated a strong significant co-existence network with other metals (e.g., Mn, Ni). Source apportionment recognized four source patterns (Cd, Pb, Ni, and Mn) for water and (Cr, Cd–Pb, Mn, and Zn) for sediment which was further confirmed by principal component analysis. The mine inputs source mainly contributed to Cd (66.07%) for water, while mineral processing mostly contributed to Zn (76.10%) for sediment. High non-carcinogenic ( $>1$ ) and carcinogenic ( $>10^{-4}$ ) health risks, particularly in children, are related to the elevated Cd, Pb and Cr contents from the VGR. Uncertainty analysis demonstrates that the 90th quantile of Cd led to higher carcinogenic risk. Pollution indices disclosed a moderate to extremely contamination status mainly along the Toko dam which poses high ecological risks identified by index calculation. However, sediment quality indicators based on probable effect levels showed that there was a 75% of likelihood that the concentrations of Cd and Pb adjacent to the VGR have a severe toxic impact on aquatic lives.

### 1. Introduction

As a vital resource, freshwater plays a crucial role in human existence, socioeconomic and environmental ecosystems (Gleeson et al., 2012; Aldieri et al., 2020). Presently, freshwater shortage and over-exploitation due to rapid urbanization and industrialization is an urgent global concern (Wang et al., 2020). In addition to this, the elevated anthropogenic inputs due to extensive mining activities have led to huge pressure on water resources in many regions, strictly limiting

sustainable development at the regional scale (Song et al., 2019; Santana et al., 2020). Therefore, study on the sustainable development and use of water resources has become a hot topic of water resource and environmental researches.

Contaminations by metals are a key environmental issue worldwide, particularly in the goldmine region (Mora et al., 2019; Vithanage et al., 2019). Elements such as Cd, Cr, Pb, Ni, Mn and Zn are considered the potential heavy metals (HMs) in the aquatic and terrestrial environments because of their existence, non-degradable and toxic

\* Corresponding author.

\*\* Corresponding author.

E-mail addresses: [towfiq\\_dm@brur.ac.bd](mailto:towfiq_dm@brur.ac.bd) (A.R.M.T. Islam), [jmallick@kku.edu.sa](mailto:jmallick@kku.edu.sa) (J. Mallick).

characteristics (Bodrud-Doza et al., 2016; Islam et al., 2020a; Khan et al., 2021). One of the potential sources of HMs is mining inputs such as the mine development, mineral processing, slum waste and tailings dam leakage (Fashola et al., 2016). HMs can also be initiated from natural sources, particularly weathering rock-water interactions (Finkelmann et al., 2018). Although some of the metals are required to the survival for human health, only trivial are needed and elevated contents might be toxic (Kumar and Trivedi, 2016). HMs like Pb, Cd and Cr are extremely hazardous at a very small amount and are less valued to human health functioning (Tchounwou et al., 2012; Jaishankar et al., 2014). Once HMs enter the human body, they deposit in vital organs including the brain, kidneys, and stomach which may be ultimately led to casualty (Jarvis and Younger, 2000; Lanocha-Arendarczyk et al., 2016). In the region where mining sites and local rural communities co-exist, HMs exposures have led to adverse impacts on the aquatic ecosystem and human health (Li et al., 2014). Recently, more attention has been paid to the exposure of HMs in the goldmine regions, intending to appraise the risks of human exposure to mine waste which is linked with their persistence and transferability in the food system (Souza et al., 2017; Hadzi et al., 2018; Pereira et al., 2020). Anthropogenic activities such as mining and dumping of mine wastes have interplayed vital roles in increasing the contents of HMs in the environment (Fashola et al., 2016). In the environment, biota such as humans is frequently exposed to more than one HM, thus facing interactive impacts (Palacios-Torres et al., 2020). Therefore, identifying the source and assessing human health risks of HMs exposure in the goldmine region is essential to expedite the combat of mitigation policies.

HMs contamination status, co-existence, source identification, ecological and human health risks appraisal, are required for developing an effective mine-derived pollution control and management strategies. Several studies have evaluated contamination level, risk assessment of metal exposure in goldmine areas worldwide (Zhang et al., 2013; Rakotondrabe et al., 2018; Mora et al., 2019; Huang et al., 2020; Capparelli et al., 2020). For instance, Souza et al. (2017) evaluated the risks of HMs through the soil, water, and plants at a goldmine region in Brazil. Sako et al. (2018) reported a comprehensive insight into the risks of HMs dispersion in soil, surface water, and groundwater around the Tongon goldmine, West Africa. Amoakwah et al. (2020) identified the source-sink relationships of HMs among soil-water-vegetative ecosystems in the Ghanaian goldmine region. Huang et al. (2020) linked the environmental and human health risks from metal exposures adjacent to a Pb–Zn–Ag mine in China. Palacios-Torres et al. (2020) assessed HMs in sediments and fish samples impacted by gold mining in Colombia. Thus, knowledge about contamination by HMs is essential to environmental and public health regulatory bodies for lessening pollution levels.

Many researchers have employed the multivariate statistical approach including principal component analysis (PCA), and factor analysis (FA) to recognize and group the various sources of metals present in surface water and sediment (Islam et al., 2015, 2020b, 2020b; Rakotondrabe et al., 2018; Khan et al., 2020). However, this approach does not report the metal source type contribution because of some limitations such as they did not explain the cause-and-effect association and data uncertainties. To report these limitations, the positive matrix factorization (PMF) model was developed by the USEPA which can efficiently deal with data uncertainties, and missing values (Hemann et al., 2009). The PMF model has been successfully used by many research scholars to get very satisfactory outcomes of source contribution types in various fields (Zanotti et al., 2019; Islam et al., 2020a; Xia et al., 2020). In our study, the PMF method was employed to water and sediment data including metals in the adjacent mine area.

Mining is an essential part of Fiji's economy and gold is one of the country's highest exports (Mines, 2019; Diarra and Prasad, 2020). Vatukoula Goldmine region (VGR), one of them, is located in the northwest Viti Levu, Fiji which was operated in the last eight decades. It encompasses 7549 ha of landmass, which has five tailings dam where all sludge waste material is deposited. Of these, the Toko tailing dam is

active and very near to the study site. However, there is a growing body of evidence that any type of tailing dam failure can cause a huge environmental disaster. The solid tailings have some sulfides mineralization like pyrite can oxidize to form an acid that can cause leaching of HMs from tailing dam and thus create a potential environmental problem (Hadzi et al., 2018; Adewumi and Laniyan, 2020). The mining activities favor the mobility of HMs and are one of the most common reasons for aquatic environmental pollution (Mora et al., 2019). In recent time, VGR has witnessed a pipeline failure along a section of the Lololevu creek and Toko tailings dam which was categorized as a truly environmental catastrophe. Few studies have reported that residents have raised their concern on high contamination of surface water, drinking water and sulfur dioxide emissions in the study region (Ackley, 2008; Matarakawa, 2018). Though many cited works on the risks of HMs via environmental media in the goldmine regions have been reported worldwide, e.g., in China (Huang et al., 2020), Brazil (Pereira et al., 2020), Nigeria (Adewumi and Laniyan, 2020), Ghana (Hadzi et al., 2018), Bolivia (Pavilonis et al., 2017), Papua New Guinea (Kapia et al., 2016). However, there is yet scarce literature on HMs contamination from the VGR in Fiji (Matarakawa, 2018). So far, no studies have been conducted to assess the baseline on human health risk or setting a baseline standard for the HMs by comparing levels from the VGR in Fiji.

In this study, we hypothesized that residents are concerned about the elevated contamination risk of HMs through surface water and sediment, and the local communities suffer from freshwater shortage and it relies on limited sources of river water for domestic purpose, and animal feeding. Because of the close vicinity of the mine to one of the key rivers in Fiji (Nasivi River), the potential mobility of mine-induced HMs to the tributaries of this river is of particular interest and deserves a thorough examination. Thus, there is an urgent need to simultaneously monitor the degree of HMs concentrations and associated risks in surface water and sediment from the VGR, to guide against the transmission of diseases and casualties. The prime objectives of this research are to determine the concentration status, and contamination level of the HMs; to explore the co-existence and potential source apportionment of the toxic metals in water resource, and to assess the ecological and human health risks associated with HMs in surface water and sediments in the VGR. The novel aspect of this work is that it is the first inclusive investigation on water resource pollution in the VGR, Fiji.

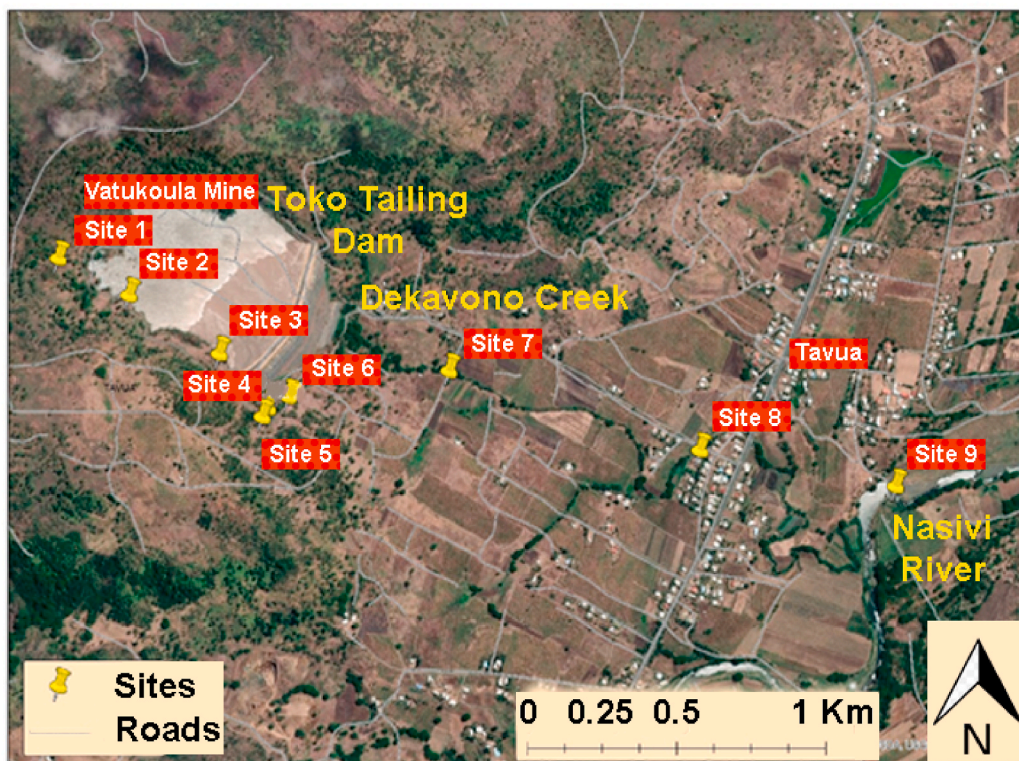
## 2. Experimental and methodologies

### 2.1. Study area specification

For studying environmental, ecological and health risks due to gold mining activities, Toko tailings dam and Dakovono creek that ends up in Nasivi River located near VGR are chosen in this work (Fig. 1a). The Toko tailings dam is utilized by the goldmine for waste disposal and is located ~3 km away from the main VGR. The Dakovono creek is the place where the effluents from the Toko tailings dam are decanted and discharged. The Dakovono creek then connects the main Nasivi River. After the gold is processed, the waste that comes as a byproduct from the mining process is pumped via pipes into the Toko-tailings dam. The Toko tailings dam is the fifth tailings dam since mining began in Vatukoula. The water from the Toko tailings dam is decanted into Dakovono creek, which finally merged with the Nasivi River. Near Toko-tailings dam, a community of people is also living and their animals drink water from the Dakovono creek.

The climate of Fiji is mainly tropical, characterized by high rainfall (2000–4000 mm) and temperature (20–30 °C) throughout the year (Mataki et al., 2006; Ongoma et al., 2021). According to Mataki et al. (2006), Fiji experiences a distinct rainfall season from November to April and a dry season is observed from May to October. The western part of the country, where the study site is located, generally records lower rainfall and higher temperatures than the central and eastern parts of the country. The VGR locates in the western part of Tavua of Viti

(a)



(b)

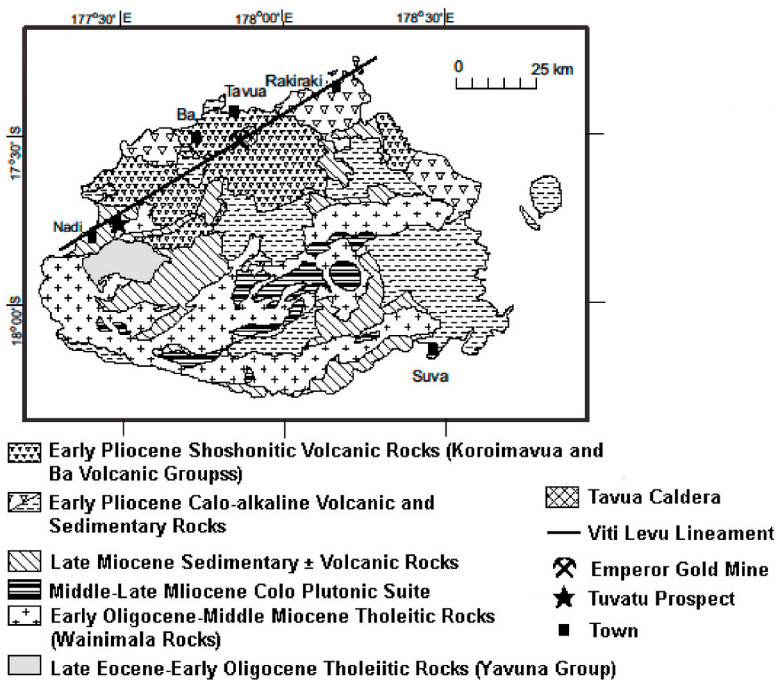


Fig. 1. Map of the study area and sampling locations. (a) Sampling sites at Toko tailings dam followed by Dakavono Creek to Nasivi River; (b) generalized geological map of Viti Levu, Fiji.

Levuisland region (Fig. 1b) where gold-telluride mineralization took place mainly in the sub-ducted fault zone.

2.2. Collection and processing of samples

Benthic sediments (SS) and surface-water (SW) samples were collected from Toko tailings dam and Dakavono creek in the vicinity of the VGR. Three sets of temporal samples (of both SW and SS) were

collected in January, May and September of 2015, respectively (cover a single hydrological calendar) from nine (09) sampling stations (1–9) as presented in Fig. 1. Total 53 samples (27 surface water and 26 sediments) were collected by 2015–2016. During the second set of sampling site 2 (SS2-2) was inaccessible, thus the sediment sample was not collected at site 2. The sampling sites were georeferenced with a GPS device (Fig. 1). Collections and preservations of samples were performed by following ISO, EPA 3050B methods with minor modifications

(Brunner et al., 2020). Briefly, water samples were collected in pre-cleaned (acid and distilled water rinsed) polyethylene bottles followed by filtering (through 0.45  $\mu\text{m}$  filter), acidification (with  $\text{HNO}_3$ ;  $\text{pH} < 2$ ) and preservation (at 4  $^\circ\text{C}$ ). During water sampling, polyethylene bottles were also rinsed by water from the studied site three times (Habib et al., 2020; Khan et al., 2021). Benthic sediments were (surface sediment: 0–10 cm depth) were collected by core-sampler and were stored in zip-lock bags with proper labeling. To obtain representative samples, 3–5 replicate samples (for both water and sediment) were collected from a single sampling station (in each temporal sampling) followed by equi-proportional mixing of them. Collected sediment samples were then dried (at 60  $^\circ\text{C}$ ), sieved (2 mm) and pulverized to obtain a homogeneous powdered sample with necessary laboratory practices to avoid cross-contaminations (Tamim et al., 2016).

### 2.3. Analytical processes and quality control

Physicochemical parameters such as pH, temperature, total dissolved solid (TDS), salinity, conductivity, dissolved oxygen (DO), and oxidation reduction potential (ORP) were determined by Horiba-52 Multimeter (Thermo Fisher Scientific, Japan) during sampling. However, heavy metal abundances in both water and sediment samples were determined by flame atomic absorption spectrometer (FAAS, PerkinElmer Analyst 400, USA) after acid digestion and required dilutions following ISO11929 protocol with minor modifications (Lymperopoulou et al., 2017). Briefly,  $\text{HNO}_3$  based acid digestion of water samples (Kabir et al., 2021) and concentrated  $\text{HNO}_3$ – $\text{HCl}$ – $\text{HF}$ – $\text{HClO}_4$  based acid digestion of sediment samples (Tamim et al., 2016) were performed followed by required dilution with double de-ionized water.

Data quality ensuring approaches including usages of properly cleaned and calibrated glassware's, double de-ionized water, analytical grade reagents, internationally recognized calibration standards (Fluka Analytical, Sigma-Aldrich, Germany), sequential measurements of procedure blanks, spiked solution mediated recovery calculations (water: 95–106%; sediment: 90.9–98.0% with  $\pm 3\%$  RSDs) were similar as those of Islam et al. (2020b) and Khan et al. (2019). Other than the linearity and robustness of analytical procedure, replicate measurements ( $n = 3$ ) of standard reference materials, such as NIST-SRM-8704 (river sediment) and NIST-SRM-1640 (natural water) were performed following the identical analytical procedures of sample measurements to ensure the accuracy and precisions of analytical data (e.g., Khan et al., 2019). Considering the analytical uncertainty, the obtained analytical data from the replicate measurements of these SRMs were well consistent with those of certificate values. RSDs for replicate measurements ( $n = 3$ ) of each SRM for each element were within  $< 10\%$ , which ensures the precision of analytical data. Detection limits calculated from the seven procedure blanks and statistical approaches (student-t test with 99% confidence limit) for Cd, Cr, Pb, Ni, Zn, and Mn were 0.010, 0.010, 0.030, 0.010, 0.010, and 0.010 mg/L, respectively.

### 2.4. Health risk appraisal, environmental and ecological indices

Non-carcinogenic health risks (NCR) in terms of hazard quotient (HQ: Islam et al., 2020b; USEPA, 2004) and hazard index (HI: USEPA, 2004) were evaluated from the estimation of the average daily dose (ADD) for ingestion ( $\text{ADD}_{\text{ingestion}}$ : Habib et al., 2020) and dermal ( $\text{ADD}_{\text{dermal}}$ : Islam et al., 2017) interaction (Table S1 and S2). On the other hand, carcinogenic health risks (CR) were estimated from the ADD and carcinogenic slope factor (SF: USEPA, 2004; Islam et al., 2020b). Furthermore, in this study, environmental indices including geo-accumulation index ( $I_{\text{geo}}$ : Muller, 1979), pollution load index (PLI: Tomlinson et al., 1980) and contamination factor (CF: Tomlinson et al., 1980) were used following the standard method (e.g., Tamim et al., 2016). However, to evaluate the sediment quality and affiliated ecological risks, probable effect level quotient (PEL-Q: Long et al., 1995), toxic unit analysis ( $\sum \text{TU}$ : Zheng et al., 2008) and potential

ecological risk index (RI: Hakanson, 1980; Khan et al., 2019; Ustaoglu and Islam, 2020) were utilized. Theoretical aspects, mathematical expressions and affiliated factors are similar to those of cited references which were further explained in the supplementary section (Text S1).

### 2.5. Statistical analyses

A robust appraisal framework was developed to understand the patterns of the distribution of HMs and detect possible sources of metals using Spearman's rank correlation-based network analysis (Islam et al., 2020a), principal component analysis (PCA: Bodrud-Doza et al., 2016) and positive matrix factorization (PMF: USEPA, 2014; Xia et al., 2020; Islam et al., 2020a) method. However, uncertainty related to carcinogenic risk can be performed into a matrix and vectors based on Monte-Carlo (MC) simulation to generate a sample output. We use the Crystal Ball software (version 11.1.2.3) for quantitative sensitivity and uncertainty analyses, and the sensitivity runs 1000 trials. A one-way ANOVA test was employed to measure significant differences among sampling sites for six HMs. Kolmogorov-Smirnov (K-S) test was used to estimate the normality and homogeneity of water and sediment datasets at the significance level of  $p < 0.05$ .

## 3. Results and discussion

### 3.1. HMs concentration variations in water and sediment

The surface water samples were slightly alkaline with mean pH of  $7.33 \pm 0.43$  (range: 6.42–7.83), which exceeded Fiji's water quality standard (MRD, 2005). The physicochemical characteristics of the surface tailing water samples are outlined in Table S3. The higher pH values were observed at all sampling points except for SW1 and SW4, which are the nearest to the study site from the Toko-tailings dam. Higher pH values might be related to the discharge of highly alkaline goldmine water and sludge waste, which can alter the chemical state of the Nasivi River (Jarvis and Younger, 2000). The temperature is relatively high with an average of  $27.22 \pm 1.56$  ( $^\circ\text{C}$ ) in the study region (range: 25.56–30.39  $^\circ\text{C}$ ). TDS, DO and EC depicted a small variation with the mean values of  $1.03 \pm 0.25$  g/L,  $6.20 \pm 1.98$  and  $1.622 \pm 0.757$  ms/cm respectively (range: 0.297–1.89 g/L, 2.89–8.25, and 0.458–2.96 ms/cm), which are much lower than MRD (2005). The salinity of the sampling points being studied is low, with an average value of  $0.822 \pm 0.392$  ppt (range: 0.2–1.5 ppt). The ORP revealed a comparatively high variation with a mean value of  $71.77 \pm 34.06$  mV (range: 20–116 mV), indicating a higher oxidation potential in the VGR.

The minimum, maximum and average values of six HMs in surface water samples from nine sampling sites in the study area are outlined in Table 1. The mean concentrations of six HMs followed in the decreasing order of  $\text{Mn} > \text{Pb} > \text{Ni} > \text{Cd} > \text{Cr} > \text{Zn}$ , which are analogous to the HMs ordering in the study by Hadzi et al. (2018) in major goldmine areas, Ghana but contrary to the toxic metals ordering in the previous work of Adewumi and Laniyan (2020) in Anka gold-mine, Nigeria.

As can be seen, the mean concentrations of Mn, Cd, and Pb were much greater than the other harmful metals. The concentration values for Ni, and Zn found in the waters of the adjacent area of VGR did not surpass the MRD (2005). However, the difference in HMs in surface water was substantial, especially Cd, Mn, Pb, which had a higher standard deviation variation than other metals (Table 1). Fig. 2a shows the spatial patterns of the HMs in the VGR of Fiji. In fact, concentrations of most HMs did not show significant temporal variations (ANOVA,  $p > 0.05$ ) in the study area.

About 100% of the samples being studied exhibited lower concentrations of Zn and Ni compared to those in MRD (2005). However, all sampling sites showed Ni concentrations greater than the WHO guideline value (0.02 mg/L). Additionally, the content of these metals in all sites was much lower than Fiji guideline values, which means that the water resource is appropriate, even for drinking (for animals). In

**Table 1**

Descriptive statistics of heavy metal (HMs) concentrations in water and sediment samples of all sites in the adjacent areas of the VGR, Fiji.

Sites		Heavy metal concentrations in water (mg/L)								
HMs		SW1	SW2	SW3	SW 4	SW5	SW6	SW7	SW8	SW9
Cd	Min	0.01	0.01	0.02	0.02	0.01	0.01	0.01	0.01	0.01
	Max	0.10	0.11	0.10	0.12	0.10	0.11	0.95	0.12	0.11
	Mean	0.06	0.07	0.07	0.08	0.06	0.07	0.35	0.08	0.07
	SD	0.05	0.05	0.04	0.06	0.05	0.06	0.52	0.06	0.05
Cr	Min	0.01	0.01	0.03	0.01	0.01	0.01	0.01	0.03	0.01
	Max	0.06	0.11	0.09	0.13	0.11	0.15	0.15	0.05	0.05
	Mean	0.03	0.06	0.06	0.06	0.04	0.06	0.06	0.04	0.03
	SD	0.03	0.05	0.03	0.06	0.06	0.08	0.08	0.01	0.02
Mn	Min	0.04	0.01	0.32	0.17	0.20	0.01	0.01	0.01	0.01
	Max	0.49	3.40	1.14	3.53	3.57	3.32	3.66	0.05	1.45
	Mean	0.25	1.27	0.64	1.81	1.47	1.27	1.24	0.03	0.55
	SD	0.23	1.85	0.44	1.68	1.83	1.79	2.10	0.02	0.79
Ni	Min	0.04	0.05	0.01	0.01	0.01	0.01	0.01	0.01	0.01
	Max	0.18	0.35	0.23	0.35	0.35	0.32	0.30	0.19	0.06
	Mean	0.09	0.15	0.10	0.13	0.12	0.14	0.14	0.07	0.04
	SD	0.08	0.17	0.12	0.19	0.20	0.16	0.15	0.10	0.03
Pb	Min	0.03	0.07	0.13	0.07	0.06	0.07	0.03	0.03	0.06
	Max	0.22	0.53	0.20	0.27	0.39	0.40	0.45	0.36	0.43
	Mean	0.10	0.25	0.16	0.16	0.18	0.20	0.20	0.16	0.19
	SD	0.10	0.25	0.04	0.10	0.18	0.18	0.22	0.18	0.21
Zn	Min	0.01	0.01	0.01	0.02	0.02	0.01	0.01	0.01	0.01
	Max	0.02	0.03	0.03	0.03	0.03	0.02	0.02	0.01	0.02
	Mean	0.01	0.02	0.02	0.02	0.03	0.02	0.02	0.01	0.01
	SD	0.01	0.01	0.01	0.01	0.01	0.01	0.01	0.00	0.01

Sites		Heavy metal concentrations in sediment (mg/kg)								
HMs		SS1	SS2	SS3	SS4	SS5	SS6	SS7	SS8	SS9
Cd	Min	7.70	3.47	12.46	3.40	6.97	4.07	3.27	3.10	2.60
	Max	14.53	15.33	13.40	12.23	16.40	19.30	18.43	13.83	23.16
	Mean	10.52	8.07	12.93	8.26	12.57	13.00	12.56	9.49	12.53
	SD	3.57	6.36	0.66	4.48	4.96	7.95	8.14	5.65	10.30
Cr	Min	6.30	15.10	150.15	7.60	5.60	6.83	0.03	18.00	8.37
	Max	120.32	132.16	302.20	73.19	181.31	74.46	90.36	181.10	337.73
	Mean	49.34	71.55	226.18	48.47	78.95	31.30	37.70	85.63	183.88
	SD	61.93	58.64	107.52	35.66	91.38	37.49	47.00	85.04	165.74
Mn	Min	38.65	84.33	7.17	31.75	2251.00	152.40	219.50	114.53	4.67
	Max	703.87	838.06	160.00	474.96	4683.33	2235.00	375.10	1203.10	739.06
	Mean	270.84	407.50	83.59	194.79	3355.22	927.57	297.30	498.71	252.09
	SD	375.34	388.17	108.07	243.72	1231.52	1138.77	110.03	610.86	421.75
Ni	Min	23.80	64.43	47.30	30.40	43.43	64.23	58.03	57.96	58.97
	Max	69.66	75.00	72.63	35.73	119.40	81.43	73.73	79.36	68.80
	Mean	41.98	70.09	59.97	32.32	74.11	70.22	67.73	68.60	64.93
	SD	24.36	5.32	17.91	2.96	40.04	9.72	8.48	10.70	5.24
Pb	Min	28.50	105.00	56.03	103.53	132.26	139.56	113.86	102.26	67.70
	Max	118.00	149.93	120.43	105.00	200.90	167.90	135.80	131.90	195.13
	Mean	70.57	130.39	88.23	104.04	162.32	153.15	124.60	116.20	128.82
	SD	44.99	23.03	45.54	0.83	35.10	14.21	10.98	14.90	63.87
Zn	Min	76.30	196.66	58.90	36.50	97.30	98.19	106.43	113.73	132.39
	Max	356.60	318.90	125.00	119.60	330.53	189.30	141.80	148.70	143.40
	Mean	170.97	246.09	91.95	80.66	187.31	147.43	120.95	127.04	138.41
	SD	160.77	64.39	46.74	41.79	125.39	46.00	18.51	18.92	5.58

general, Ni and Zn may be enriched naturally in the study region (Bokar et al., 2020). The concentration above Cr levels reported by Fiji and international laws was found in 66.66% of surface water samples. Additionally, six sampling sites surpassed the recommended value of Cr (0.05 mg/L). The high concentration of Cr found at SW-02 and SW-06 (0.06 mg/L) can be explained by the fact that these sites are between Toko tailings-dam and Dakovono-creek e.g., near goldmine sludge area. A plausible source of Cr in these sites may be dissolved in ultramafic volcanic rock by weathering and diagenesis processes, which led to the elevated content (Zhitkovich, 2011).

As stated in Table 1, Mn was an abundant metal in surface water (MRD, 2005). All samples of surface water in which Mn was identified (88.89%) exhibited elevated contents, being the average value: 0.95 mg/L, 9.5 times the WHO (2017) suggested values. Also, SW-04 and SW-05 also showed 18.1 and 14.7 times higher than the WHO (2017) and Fiji standard values (0.10 mg/L). The highest concentrations of Mn (1.81 mg/L) were found in SW-4, which is 3 km apart from the study

mine due to the secondary effect. This site is near the dumping edge of the Toko-tailings dam. The exploitation of precious stones, which are indebted its purple tone to impurities of a transition metal like Mn, may likely be the key reason why the content of Mn found in this sample was 1.9 times higher than the average content in the adjacent area of the VGR. Overall, high Mn content was found near the mine area (SW-02, SW-04 and SW-06). Further, the current climatic setting in this region supports Mn transport in the form of manganese hydroxide by forming carbonate strata (Maata and Singh, 2008). While pH values from 6.62 to 7.83 in most of the water samples, the solubility of Mn tends to enhance (Islam et al., 2020b). Based on this evidence, elevated Mn concentrations found in surface waters may have a geogenic origin, associated with chemical weathering and dissolution of ore in the bedrocks. The highest concentration values of Cd and Mn were found at SW-04 (1.81 mg/L), SW-07 (0.25 mg/L), respectively, in water resources (SW-07), nearly 3 km far away from the goldmine (Table S4). Surprisingly, the elevated values of Pb, and Ni were detected at SW-02 and SW-06, which

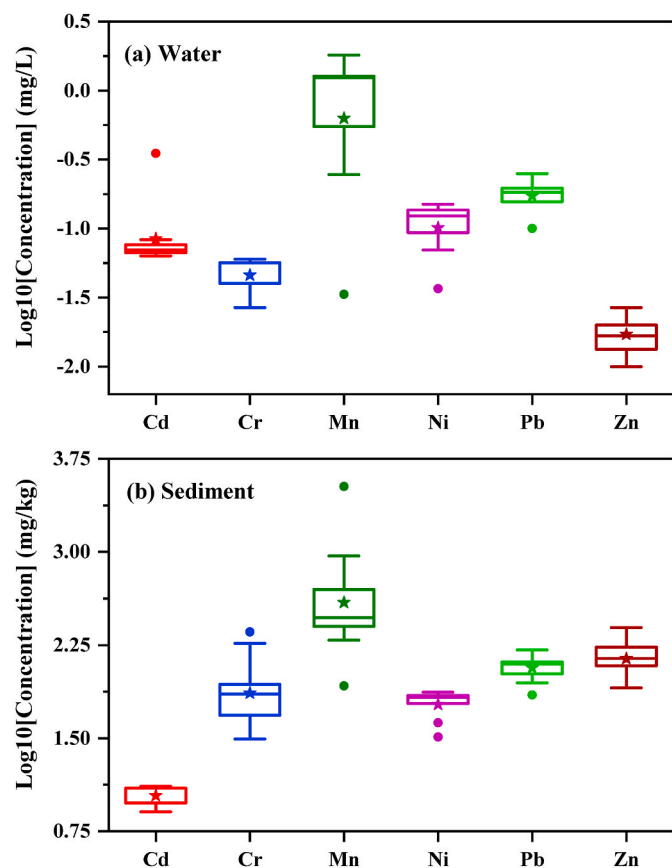


Fig. 2. Box-and-Whisker plots of HM concentrations for water (mg/L) and Sediment (mg/kg) samples. Boxes represent the 25th, 50th and 75th percentile, bars show the maximum and minimum, stars show mean, and circles show outliers data.

are near the Toko-tailings dam from the mine mineral processing area. Approximately 100% of surface water samples showed Cd levels greater than 0.04 mg/L, which is the guideline value for freshwater of Fiji water quality standard, and all sampling sites also surpassed the reference value set by WHO (2017). The key source of water contamination by Cd is mining activities, mostly of non-ferrous metals. Nevertheless, the deposition of waste material in the rocks, the discharge of sludge, Ni–Cd batteries and agrochemical input are also vital sources of contamination (Arikibe and Prasad, 2020). The effect of human inputs would elucidate the elevated contents of Cd in the water samples analyzed, particularly in the samples near the mine regions (SW-01 to SW-07).

Of all HMs analyzed, the concentrations of Cd and Pb in the surface water samples examined were the most concerning, due to their toxicity impacts. Cadmium is an extremely toxic metal, thus, its existence in the elevated contents in water samples poses a severe risk to aquatic lives. Similarly, Pb poisoning is associated with different diseases of the nervous scheme, kidney loss and behavioral disorders in children. Both Pb and Cd are demarcated as likely human carcinogenic effects and are related to skeletons, lung and stomach cancer risks (Jarup, 2003). The average value of Pb in all samples of surface water being studied (0.18 mg/L) surpassed the acceptable levels set by the WHO (2017) (Table 1). Nearly 88.89% of the water samples exceeded these permitted levels except for SW1. The temporal changes found in the concentration of Pb across the VGR indicate diverse contamination, implying that mining may not solely contaminate the source pathway. It has been stated that waste material originated from gold mining involves, among other toxic elements, a high content of Pb, which can be simply moved by waste effluents and acid drainage, hence reaching the soil surface and surface water near the mine area (Fernandes et al., 2004). As a result, it assumed

that this was probably contributed to the dilution and flushing effect by the natural discharge of the river (Morrison et al., 2001). The results of this study reveal that very high concentrations of Pb and Cd loaded from the mining wastewaters that discharged into Nasivi Rivers, have led to the degradation of the rivers water quality. Furthermore, the concentrations of toxic HMs in the mining wastewaters are yet very high and the deposition of pollutants could represent a vital source of toxicity for the aquatic food chains as well as for the riverine people. Thus, the possible adverse impacts of mining pollution should be examined and constantly monitored to inhibit extensive and hazardous contamination by HMs and to preserve the freshwater resource that is highly influenced by the widespread mining inputs.

The comparison of selected HMs in the analyzed water samples with other goldmine areas in Fiji and worldwide is shown in Table 2. The mean HM's concentrations in the VGR were much greater than the world average, except for Ni, and Zn. Compared with other countries, Cd and Pb contents in the study sites were larger than those in the Betare-Oye goldmines, Cameroon (Rakotondrabe et al., 2018), the major goldmine, Ghana (Hadzi et al., 2018), and lower than that in the Anka goldmine, Nigeria (Adewumi and Laniyan, 2020). The average Cr content was higher than those in the Betare-Oye goldmines, Cameroon (Rakotondrabe et al., 2018), and Jiaodong goldmine, China (Zhang et al., 2013) but lower than those in major goldmine, Ghana (Hadzi et al., 2018). It can be said that VGR indicated relatively higher pollution contents except for Ni, and Zn, even other goldmine areas worldwide with severe impacts of mining activities (Santana et al., 2020).

The minimum, maximum and average values of six HMs in sediment samples from nine sampling sites in the study area are displayed in Table 1. The mean concentration of six HMs decreased in the following order Mn > Zn > Pb > Cr > Ni > Cd, which is alike to the toxic metal ordering in the study by Mora et al. (2019) in Nambija goldmine, Equador. From the outcomes of the spatial pattern, it is obvious that Pb and Cd exhibited significant differences among sampling sites ( $p < 0.05$  by ANOVA and KS-test) demonstrating the effect of anthropogenic inputs in the study region (Fig. 2b). Mn concentrations followed a trend of almost the upper continental crust (UCC) value (775 mg/kg) and the average shale value (850 mg/kg). However, it is elevated in SS5 (3344.22 mg/kg), where all sludges from the VGR are deposited. The high contents of Mn in sediment may possess a lithogenic origin (Islam et al., 2015). Averages of Mn in sediments were lower than their corresponding average shale value (ASV) concentrations, whereas Zn was 1.53 times higher than the respective ASV concentrations. The Zn values exceeded the UCC (67 mg/kg) and ASV (95 mg/kg) and the threshold effect level (TEL) value (124 mg/kg) in all locations. The increase in Zn at sampling sites SS5, and SS6 may contribute to galvanizing product when cyanide may be associated with gold mineral processing as a leaching gold from ore. This outcome agrees with the results of Song et al. (2019) who found higher concentrations of Zn in the sediment of Zhaoyuan goldmine, China.

The mean Pb values surpassed the ASV (20 mg/kg), UCC (17 mg/kg) and potential effect level (PET) value (112 mg/kg) at all sampling sites, though the elevated Pb concentrations were found in SS5 (162.32 mg/kg), SS6 (153.15 mg/kg), SS2 (130.38 mg/kg) and SS9 (128 mg/kg). The rise in Pb value may be attributed to vehicle traffic emission derived from the study area highway, which often passes over the sampling sites, atmospheric deposition on the roadside (Pratap et al., 2020). Compared with the ASV, mean concentrations of Cd, and Pb in sediment samples of the VGR surpassed the ASV levels (Table 2) which were 37, and 5.99 times higher than their respective ASV concentrations. In this study, the maximum concentrations of Pb, and Cd were identified at sampling sites SS5 and SS6, which receive wastewater sludge discharges from the Toko-tailing dam edge. These outcomes suggest that Cd and Pb in sediments of the VGR were controlled by anthropogenic inputs. It clearly demonstrates that the VGR is heavily polluted by mining inputs which could induce significant environmental effects and potential health risks. The local authority and the mining operators should hence

**Table 2**

Heavy metals (HMs) abundances in water and sediment samples from VGR, Fiji compared with those in relevant literature works as well as with the internationally recognized limit values.

Gold Mines	Cd	Cr	Mn	Ni	Pb	Zn	References
<b>Water</b>							
Vatukoula Gold Mine, Fiji	0.10	0.05	0.95	0.11	0.18	0.02	This study
Anka Gold Mines, Nigeria	1.20	0.06	0.38	6.53	0.06	0.03	Adewumi and Laniyan (2020)
Bétaré-Oya Gold Mines, Cameroon	0.05	0.02	0.10		0.10	0.40	Rakotondrabe et al. (2018)
Major Gold Mines area, Ghana		0.11	1.48	0.11	0.01	0.07	Hadzi et al. (2018)
Andean Gold Mines, Ecuador	0.02	0.27	2.97	0.15	0.14	0.79	Capparelli et al. (2020)
Roşia Montană Gold Mines, Romania	0.04		51.97		0.06	5.63	Florea et al. (2005)
Ilesha gold mines, southwest Nigeria		0.00	0.13	0.01	0.01	0.07	Odukoya et al. (2017)
Gauteng Gold Mines, South Africa		0.14		0.39	0.01	0.33	Kamunda et al. (2018)
Linglong Gold Mining Area, China	0.03	0.01			0.07	1.01	Ning et al. (2011)
Jiaodong Gold Mines, China	0.04	0.03	0.01		0.40	2.52	Zhang et al. (2013)
WHO	0.003	0.05	0.10	0.02	0.01		WHO (2017)
Fiji Standards	0.004	0.05	0.10	0.20	0.10	5.00	Mineral Resources Department (2005)
FAO (Irrigation) Standards	0.01	0.10	0.20	0.20	5.00	2.00	FAO (2003)
BIS Standards	0.003		0.10	0.02	0.01	5.00	BIS (2012)
EPA Standards	0.005	0.05	0.05	0.02	0.05	3.00	EPA (2005)
<b>Sediment</b>							
Vatukoula Gold Mines, Fiji	11.10	90.33	698.62	61.10	119.81	145.64	This study
Anka Gold Mines, Nigeria	0.10	111.82		39.20	2234.02	42.55	Adewumi and Laniyan (2020)
Zhaoyuan City Gold Mines, China	36.30	35.80			65.80	297.60	Song et al. (2019)
Marahiq Gold Mines, Egypt	0.15	27.93		22.30	8.37	60.57	Darwish (2017)
Selinsing gold mine, Malaysia	0.02	2.19	61.66	1.64	2.38	9.99	Kusin et al. (2019)
Nambija Gold Mines, Ecuador		12.25	1674.43	10.68	132.74	484.84	Mora et al. (2019)
Andean Gold Mines, Ecuador	3.15	14.65	480.75	10.70	3.55	41.05	Capparelli et al. (2020)
Morila Gold Mines, Mali	0.01	66.00	222.00	6.46	12.80	11.80	Bokar et al. (2020)
Migori-Transmara Gold Mines, Kenya	0.25	63.05		89.28	130.20	99.70	Odumo et al. (2018)
Kedougou Gold Mines, Senegal		396.39		61.50	16.39	100.43	Niane et al. (2014)
ABA Gold Mines, Côte d'Ivoire <sup>a</sup>	36.80	33.50	189.00	29.70	77.80	91.20	Kinimo et al. (2018)
Choco Gold Mines, Colombia	0.22	163.20		55.20	5.62		Palacios-Torres et al. (2020)
Jiaodong Gold Mines, China	4.10	339.00			167.00	639.00	Zhang et al. (2013)
Upper continental crust (UCC) value	0.09	92	775	47	20	67	Rudnick and Gao (2014)
ASV <sup>f</sup>	0.3	90	850	68	17	95	Islam et al. (2020a)
ERL <sup>b</sup>	1.2	81		20.9	46.7	150	Long et al. (1995)
ERM <sup>c</sup>	9.6	370		51.6	218	410	Long et al. (1995)
TEL <sup>d</sup>	0.68	52.3		15.9	30.2	124	MacDonald et al. (2000)
PEL <sup>e</sup>	4.21	160		42.8	112	271	MacDonald et al. (2000)

<sup>a</sup> ABA: Agbaou, Bonikro and Afema Gold Mines.

<sup>b</sup> ERL: Effective Range Low.

<sup>c</sup> ERM: Effective Range Median.

<sup>d</sup> TEL: Threshold Effect Level.

<sup>e</sup> PEL: Probable Effect Level.

<sup>f</sup> ASV: Average Shale Value).

immediately establish the wastewater treatment plant before discharging the mine wastes into the aquatic ecosystem.

Generally, the values of Ni often did not surpass the ASV (68 mg/kg), except for some sites SS5, SS6, and SS2. Earlier studies stated that Ni is originated from geogenic sources (Xue et al., 2014), which is comparable to the UCC (46 mg/kg) in the study region. Mineral comprising Cr like chromite [(Fe,Mg,Al)Cr<sub>2</sub>O<sub>4</sub>] is common in rock and soil particles while atmospheric deposition and mining sludge are the other sources (Tamim et al., 2016; Khan et al., 2020). The mean concentration of Cr did not surpass the ASV (90 mg/kg) and PEL (160 mg/kg) at all sampling points, except for few sites SS3 and SS9. Cr concentrations were recorded as 226 mg/kg (SS3) and 183 mg/kg (SS9) that exceeded the PEL value in Toko-tailing dam proximal side and the Nasivi River where gold mining processing plant and agricultural activities are severe. Varol (2020) stated that effluents from mineral processing areas have elevated Cr levels. In our study, all values of Cd were observed to be higher than ASV (0.3 mg/kg). The elevated Cd concentration in sediment may be contributed to human activities such as extensive gold mining, refining

and welding (Pandey et al., 2019). Habib et al. (2020) stated that wastewater discharge from mine power plant triggers Cr and Cd enrichment in the Barapukuria coal mine of Bangladesh, which is similar to this study.

The mean values of Pb, and Cd in sediments from this study were higher than those found in Marahiq goldmine, Egypt (Darwish et al., 2017) and Andean goldmine, Ecuador (Capparelli et al., 2020). The mean values of Zn and Mn in this study were comparable to those previously reported in the Nambija goldmine, Ecuador (Mora et al., 2019). Comparison of HMs concentrations in sediments of the VGR with the cited works of other goldmines in Fiji and other countries depicted that sediments of the study area were heavily polluted (Table 2). The level of mean HMs contamination in the VGR was comparable to that in the Migori-Transmara goldmine in Kenya and Zhaoyuan city goldmine in China, but much worse than that in Marahiq goldmine in Egypt, and Choco goldmine in Colombia.

### 3.2. Co-existence correlation network in water and sediment

In this work, PCA was employed for total HMs concentrations and four components were recognized for both water and sediment based on their eigenvalues that elucidated 95.47% and 92.13% of the total variance, respectively (Table S5 and Fig. 3). For water, Mn and Zn had a high positive loading on PC1 (57.75% of total variance), suggesting that both metals surely come from a combination of natural and anthropogenic sources within the study region (Fig. 3a).

Like the spatial pattern was identified in earlier studies (Santana et al., 2020). Cr and Ni showed a high positive loading on PC2 (18.64%), suggesting these metals were originated from geogenic material influence by mine inputs (Xue et al., 2014) whereas Pb and Cd had an elevated positive loading on PC3 and PC4 (11.95% and 7.11% of the total variance), indicating these PC could be associated to goldmine and mineral processing activities.

On the other hand, for sediment, Pb and Ni had a high positive loading on PC1 (44.46% of total variance), indicating a diverse source in the adjacent area of a goldmine (Fig. 3b). Previous works were found a diverse spatial distribution (Mora et al., 2019). Elevated positive loading on PC2 (26.5%) and PC3 (13.31%) was observed for Mn and Zn, indicating while high negative loading on PC3 was found in Cd. Cr had a high loading on PC4.

To further appraise the likely sources among HMs in water and sediment, we performed a co-occurrence correlation network (CCN) based on Spearman's correlation analysis ( $>0.50$ ,  $p < 0.01$ , Fig. 4). For water, Cd was excluded from the CCN because of the weak or insignificant relationships with other HMs. The significant co-occurrence relationships were measured among HMs, particularly for Pb, Ni, Cr and Mn (Fig. 4a). Nickel exhibited comparatively strong co-occurrence relationships with Cr ( $r = 0.89$ ,  $p < 0.01$ ) and Pb ( $r = 0.69$ ,  $p < 0.01$ ), thus indicating that those have common sources. Chromium and Pb had analogous co-existence relationships ( $r = 0.68$ ,  $p < 0.01$ ), which suggested similarities in the pattern of these pollutants affecting the extensive mining influence from the VGR. Zinc exhibited weak co-occurrence relationships with Mn ( $r = 0.87$ ,  $p < 0.01$ ). This could be contributed to the geogenic source in the study sites (Zanotti et al., 2019). However, Cd did not exhibit any association with other HMs. Cadmium possibly comes from anthropogenic sources as already discussed.

For sediment, Cr, Zn and Cd were excluded from the CCN due to their low or non-significant associations with other HMs (Fig. 4b). Nickel had strong co-existence associations with Pb ( $r = 0.088$ ,  $p < 0.01$ ) and Mn ( $r = 0.90$ ,  $p < 0.1$ ), likely the idea of a similar source. Hydrated oxides of Mn might be related to other metals when Mn comprises potential sinks

for Pb, Ni in the aquatic ecosystem, especially under oxidation circumstances (pH 6.42–7.83) (Venkatramanan et al., 2015). This is a basic physicochemical procedure of adsorption and co-precipitation conditions. Lead showed a similar co-occurrence association with Mn ( $r = 0.75$ ,  $p < 0.05$ ).

### 3.3. Quantifying HMs apportioning sources in water and sediment

The HMs contents and their uncertainty were applied as input metal contents to the PMF method. The outcome of the PCA revealed that the optimal number of factors to appropriately represent the VGR is four. Generally, the first 4 factors were eco-environmentally interpretable in this work. After 100 runs of the PMF method, the number of source factors was set to four. Four factors were recognized as the best number of source factors for the analyzed datasets based on the lowest Q values and highest  $r^2$  values between the predicted and estimated metal contents.

Predicted metal contents were compared with the estimated metal contents using the PMF method (Fig. S1). The coefficients of determination ( $r^2$ ) values were used to evaluate the ability of the PMF method predictions. All HMs exhibited a reasonably high linear regression outcome with  $r^2$  values higher than 0.58 for water and 0.59 for sediment ( $p < 0.01$ ). The elevated  $r^2$  values were observed for Cd (1.00), Mn (1.00), Ni (0.99), Pb (0.97), and Cr (0.81), respectively for water and Cr (0.99), Mn (0.99), Zn (0.99), Pb (0.89) and Ni (0.85), respectively for sediment; indicating the studied datasets predicted were well elucidated in the PMF method.

The PMF method results for factor contributions are outlined in Fig. 5. For water, factor 1 (FC1) was highly explained by Cd with a 66.07% strong contribution, which was similar to PC4 (Fig. 5a). Factor 2 (FC2) was moderately characterized by Pb (44.61%), Cr (42.92%) and Ni (39.87%) contributions, respectively. Lead had a medium FC2 contribution, which was alike to PC3. Factor 3 (FC3) also had a moderate contribution from Ni (52.54%) and Mn (49.05%). Nickel was explained by FC3 in the PMF method, and exhibiting high positive loading on PC2. Factor 4 (FC4) was represented by medium contribution like Mn (50.32%) and Pb (44.44%) respectively which is analogous to PC1. Cadmium was predominantly contributed by a sole factor while Cr and Ni exhibited analogous source components. In general, the results of PCA are in accord with PMF analysis. For instance, the elevated levels of Pb, Cr and Ni in FC2 of the PMF analysis are also supported by a significant association of Pb with Cr ( $r = 0.682$ ,  $p < 0.01$ ), Pb with Ni ( $r = 0.698$ ,  $p < 0.01$ ), Cr with Ni ( $r = 0.894$ ,  $p < 0.01$ ) demonstrating the similar source apportionment in the VGR. The plausible source of Cr in surface water points may originate from ultramafic volcanic rock

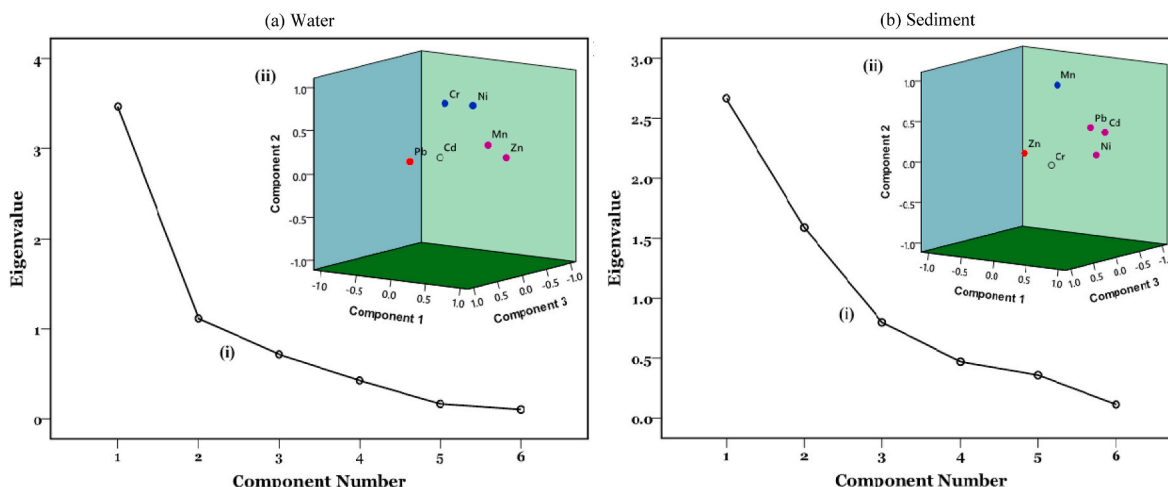


Fig. 3. Principal component analysis (PCA) of HMs in (a) water and (b) sediment samples. (i) Scree plot; (ii) rotated matrix component in the VGR.

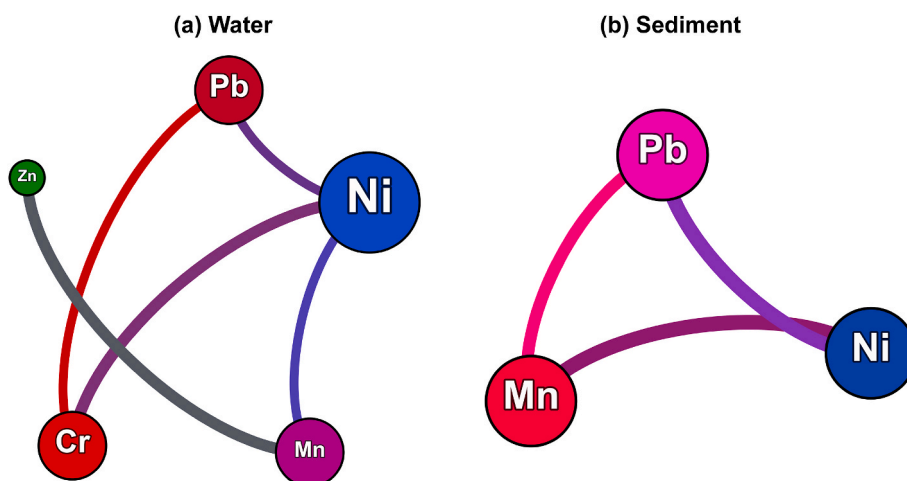


Fig. 4. Co-occurrence correlation network of HMs variation profiles at spatiotemporal scale in sediment of the VGR. Nodes characterize potentially harmful metals where the connection of each node discloses correlation coefficient between them. The size of each node is proportional to the number of connections (e.g., degree) and the thickness of each connection between two nodes (e.g., edge) is proportional to the value of Spearman’s correlation coefficient ( $\rho > 0.5$  and  $p < 0.05$ ).

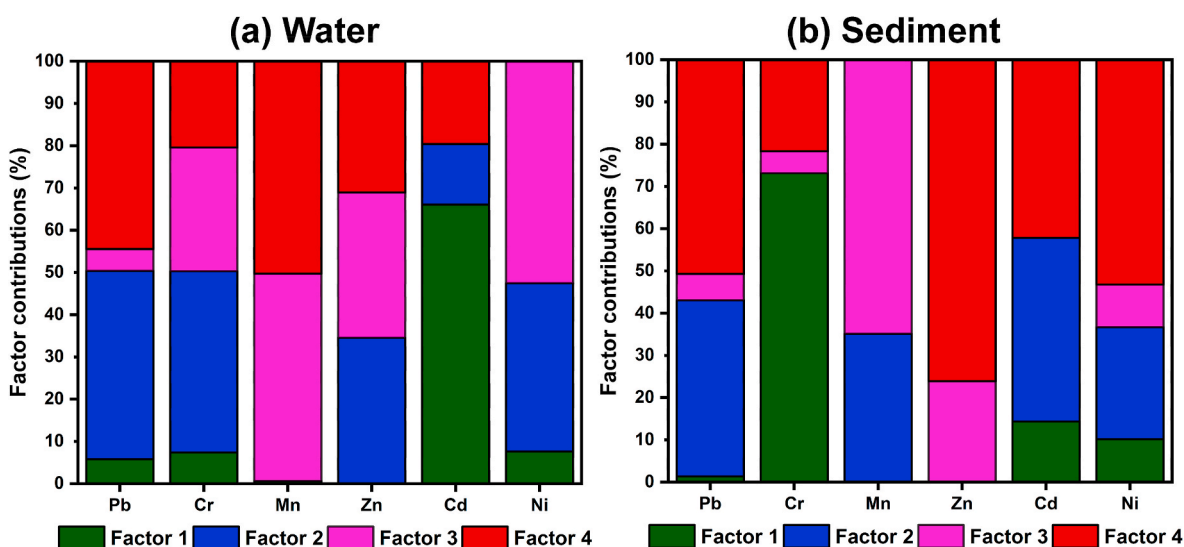


Fig. 5. Contribution of four apportioning factors water and sediment in each HM determined by the PMF method.

dissolved by weathering and diagenesis processes that led to dangerous levels (Adewumi and Lanjyan, 2020). Hence, FC1 is most possibly predominated by anthropogenic contribution while FC2 is dominated by a combination of geogenic and anthropogenic sources (Zhaoyong et al., 2015). The lead derives from the exhaust pipes of duty big trucks, vehicles and mining-related machinery maintaining patches (Armah et al., 2010) and Cd results from the Ni–Cd batteries that are used in goldmine processing locations. The elevated contents of Ni with Mn in FC3 are also confirmed by a significant association of Ni with Mn ( $r = 0.683$ ,  $p < 0.01$ ), indicating a natural parent rock-water interaction sources such as weathering and erosion from adjacent mine areas (Huang et al., 2020; Islam et al., 2019). The geological features of the study region, which is rich in gold deposits, confirm the high availability of Mn in surface water. Similarly, the medium levels of Mn and Pb in FC4 are also supported by moderate associations ( $r = 0.462$ ,  $p < 0.05$ ), suggesting a mixed source. Generally, Mn and Pb are mainly leached from tailing dam waste, goldmine materials and products used during the operation (Rakotondrabe et al., 2018). Zinc showed inconsistent outcomes with low weighting in PMF FC2 analysis contrasting with high loading in PC1.

As can be seen in Fig. 5b, in the case of sediment, FC1 was characterized by Cr with a strong contribution (73.11%). FC2 was moderately

elucidated by Cd (43.44%) and Pb (41.68%). Cadmium had a medium contribution to FC2. FC3 had a strong contribution from Mn (64.89%). FC4 exhibited a high contribution to Zn (76.10%) which was similar to PC3. Nickel and Pb showed medium contribution by FC4 of 53.25%, and 50.72%, respectively. The results of PMF analysis exhibited a common source pattern in Ni and Pb, whereas Cr and Mn had similar factors in their source apportionment. However, Cd was initially attributed to a sole factor. In fact, the outcomes of PCA were in line with the results of PMF analysis. FC1 most possibly had a dominant lithogenic origin in the sediment (Santos et al., 2020). Chromium in the study area denotes a risk of contamination to the biota and the local resident because its hexavalent form possesses a high carcinogenic risk. FC3 likely had been characterized by natural parent material of the soils, deposited in sediment column via different geogenic events such as the disintegration of rock particles near mining waste in the study region. Similar outcomes were also detected for Ni and Pb, which exhibit very high loading on PC1 and high weighting in FC4 of the PMF modeling. In PC3, Cd and Zn showed relatively high loadings of PCA in comparison with the very weighting of PC2, and PC4 indicated a dissimilar source. Cadmium showed predominated moderate contribution by FC2 in PMF analysis and represented a high negative loading on PC3, indicating an

anthropogenic source compared to other HMs. Cadmium results from welding, automobile exhaust and batteries (Islam et al., 2015, 2020a, 2020a). Lead also exhibited a comparatively high weighting with FC2. Earlier studies have observed that Pb is initially derived from vehicle traffic point source those are located in the urban region (Xia et al., 2020). Nickel comes from the Ni battery that is used in mine processing time. Furthermore, high Zn content in sediment may be attributed to the ecological emission from vehicles, particularly tire wear in mining sites. Another source of Zn has galvanized product when cyanide might be associated with gold processing as a leaching gold from ore. Thus, FC4 is likely predominated by a diverse combination of origins.

### 3.4. Health risk assessment of HMs in water

So far, this is the first inclusive study that reported on the potential health risk for the local inhabitants adjacent to the VGR in Fiji. Table 3 shows the results of HQ ingestion, HQ dermal, and HI values in the study area. Overall, in the case of non-carcinogenic risk, HI values for both age populations surpassed the safe range (>1) in all sites (Table S6), implying that the surface water from the study area exhibited an obvious potential health risk. The HQ's values of adults were more than 1 with their respective average values of 5.58,  $4.36 \times 10^{-1}$ ,  $5.64 \times 10^{-1}$ ,  $1.50 \times 10^{-1}$ , 3.46, and  $1.62 \times 10^{-3}$ , for Cd, Cr, Mn, Ni, Pb and Zn, respectively. Similar to children, the HQ's value (>1) was followed by the mean values of 13.02, 1.02, 1.32,  $3.49 \times 10^{-1}$ , 8.07, and  $3.79 \times 10^{-3}$ , respectively. The HQ of the ingestion route peaks for Cd and reaches its minimum level for Zn regardless of both age populations. The HQ dermal values of HMs were found similar results, suggesting that the studied HMs presented adverse health hazards via the dermal route. However, children had a much greater value of non-carcinogenic risk than adults, though these are exposed to an alarming rate in the study region. The main reason is that Cd, Pb, and Cr play a crucial role in triggering high non-carcinogenic risk for children than adults. Among these HMs, HQ ingestion and dermal and HI values of Cd, Pb and Cr in water resources were extreme, indicating their adverse health effects on local inhabitants.

Overall, the total HI of non-carcinogenic risk from six HMs is 2.5

**Table 3**  
Non-carcinogenic health risk and carcinogenic risk of the analyzed HMs in the surface water samples collected from the adjacent areas of VGR, Fiji.

HMs	Non-carcinogenic Risks				HI = ΣHQs		Carcinogenic Risks (CR)				
	HQ <sub>ingestion</sub>		HQ <sub>dermal</sub>		Adult	Child	CR <sub>ingestion</sub>		CR <sub>dermal</sub>		
	Adult	Child	Adult	Child			Adult	Child	Adult	Child	
Cd	Min	3.47	8.10	1.81	5.34	5.28	13.44	$6.59 \times 10^{-4}$	$1.54 \times 10^{-3}$	$1.36 \times 10^{-4}$	$4.01 \times 10^{-4}$
	Max	19.18	44.75	10.01	29.53	29.19	74.28	$3.64 \times 10^{-3}$	$8.50 \times 10^{-3}$	$7.51 \times 10^{-4}$	$2.22 \times 10^{-3}$
	Mean	5.58	13.02	2.91	8.59	8.49	21.62	$1.06 \times 10^{-3}$	$2.47 \times 10^{-3}$	$2.18 \times 10^{-4}$	$6.45 \times 10^{-4}$
	SD	5.11	11.93	2.67	7.87	7.78	19.80	$9.71 \times 10^{-4}$	$2.27 \times 10^{-3}$	$2.00 \times 10^{-4}$	$5.90 \times 10^{-4}$
Cr	Min	$2.44 \times 10^{-1}$	$5.68 \times 10^{-1}$	$1.27 \times 10^{-1}$	$3.75 \times 10^{-1}$	$3.71 \times 10^{-1}$	$9.43 \times 10^{-1}$	$3.65 \times 10^{-4}$	$8.52 \times 10^{-4}$	$3.75 \times 10^{-4}$	$3.75 \times 10^{-4}$
	Max	$5.48 \times 10^{-1}$	1.28	$2.86 \times 10^{-1}$	$8.44 \times 10^{-1}$	$8.34 \times 10^{-1}$	2.12	$8.22 \times 10^{-4}$	$1.92 \times 10^{-3}$	$1.92 \times 10^{-3}$	$1.92 \times 10^{-3}$
	Mean	$4.36 \times 10^{-1}$	1.02	$2.28 \times 10^{-1}$	$6.72 \times 10^{-1}$	$6.64 \times 10^{-1}$	1.69	$6.54 \times 10^{-4}$	$1.53 \times 10^{-3}$	$1.53 \times 10^{-3}$	$1.53 \times 10^{-3}$
	SD	$1.20 \times 10^{-1}$	$2.80 \times 10^{-1}$	$6.26 \times 10^{-2}$	$1.85 \times 10^{-1}$	$1.82 \times 10^{-1}$	$4.64 \times 10^{-1}$	$1.80 \times 10^{-4}$	$4.19 \times 10^{-4}$	$4.19 \times 10^{-4}$	$4.19 \times 10^{-4}$
Mn	Min	$1.99 \times 10^{-1}$	$4.63 \times 10^{-2}$	$2.59 \times 10^{-3}$	$7.64 \times 10^{-2}$	$2.24 \times 10^{-2}$	$5.40 \times 10^{-2}$	$2.24 \times 10^{-2}$	$5.40 \times 10^{-2}$	$2.24 \times 10^{-2}$	$5.40 \times 10^{-2}$
	Max	1.08	2.51	$1.40 \times 10^{-1}$	$4.14 \times 10^{-1}$	1.22	2.93	1.22	2.93	1.22	2.93
	Mean	$5.64 \times 10^{-1}$	1.32	$7.36 \times 10^{-2}$	$2.17 \times 10^{-1}$	$6.38 \times 10^{-1}$	1.53	$6.38 \times 10^{-1}$	1.53	$6.38 \times 10^{-1}$	1.53
	SD	$3.58 \times 10^{-1}$	$8.35 \times 10^{-1}$	$4.67 \times 10^{-2}$	$1.38 \times 10^{-1}$	$4.04 \times 10^{-1}$	$9.73 \times 10^{-1}$	$4.04 \times 10^{-1}$	$9.73 \times 10^{-1}$	$4.04 \times 10^{-1}$	$9.73 \times 10^{-1}$
Ni	Min	$5.02 \times 10^{-2}$	$1.17 \times 10^{-1}$	$1.31 \times 10^{-3}$	$3.87 \times 10^{-2}$	$5.15 \times 10^{-2}$	$1.21 \times 10^{-1}$	$5.15 \times 10^{-2}$	$1.21 \times 10^{-1}$	$5.15 \times 10^{-2}$	$1.21 \times 10^{-1}$
	Max	$2.05 \times 10^{-1}$	$4.79 \times 10^{-1}$	$5.36 \times 10^{-2}$	$1.58 \times 10^{-2}$	$2.11 \times 10^{-1}$	$4.95 \times 10^{-1}$	$2.11 \times 10^{-1}$	$4.95 \times 10^{-1}$	$2.11 \times 10^{-1}$	$4.95 \times 10^{-1}$
	Mean	$1.50 \times 10^{-1}$	$3.49 \times 10^{-1}$	$3.91 \times 10^{-2}$	$1.15 \times 10^{-2}$	$1.54 \times 10^{-1}$	$3.61 \times 10^{-1}$	$1.54 \times 10^{-1}$	$3.61 \times 10^{-1}$	$1.54 \times 10^{-1}$	$3.61 \times 10^{-1}$
	SD	$5.14 \times 10^{-2}$	$1.20 \times 10^{-1}$	$1.34 \times 10^{-2}$	$3.96 \times 10^{-2}$	$5.28 \times 10^{-2}$	$1.24 \times 10^{-1}$	$5.28 \times 10^{-2}$	$1.24 \times 10^{-1}$	$5.28 \times 10^{-2}$	$1.24 \times 10^{-1}$
Pb	Min	1.96	4.57	$3.41 \times 10^{-2}$	$1.00 \times 10^{-2}$	1.96	4.58	$2.33 \times 10^{-5}$	$5.43 \times 10^{-5}$	$1.22 \times 10^{-8}$	$3.59 \times 10^{-8}$
	Max	4.89	11.4	$8.51 \times 10^{-2}$	$2.51 \times 10^{-2}$	4.90	11.4	$5.82 \times 10^{-5}$	$1.36 \times 10^{-4}$	$3.04 \times 10^{-8}$	$8.97 \times 10^{-8}$
	Mean	3.46	8.07	$6.02 \times 10^{-3}$	$1.77 \times 10^{-2}$	3.46	8.08	$4.11 \times 10^{-5}$	$9.60 \times 10^{-5}$	$2.15 \times 10^{-8}$	$6.34 \times 10^{-8}$
	SD	$8.00 \times 10^{-1}$	1.87	$1.39 \times 10^{-2}$	$4.10 \times 10^{-2}$	$8.01 \times 10^{-1}$	1.87	$9.52 \times 10^{-6}$	$2.22 \times 10^{-5}$	$4.97 \times 10^{-9}$	$1.47 \times 10^{-8}$
Zn	Min	$9.13 \times 10^{-4}$	$2.13 \times 10^{-3}$	$2.86 \times 10^{-6}$	$8.44 \times 10^{-6}$	$9.16 \times 10^{-4}$	$2.14 \times 10^{-3}$	$9.16 \times 10^{-4}$	$2.14 \times 10^{-3}$	$9.16 \times 10^{-4}$	$2.14 \times 10^{-3}$
	Max	$2.44 \times 10^{-3}$	$5.68 \times 10^{-3}$	$7.63 \times 10^{-6}$	$2.25 \times 10^{-5}$	$2.44 \times 10^{-3}$	$5.70 \times 10^{-3}$	$2.44 \times 10^{-3}$	$5.70 \times 10^{-3}$	$2.44 \times 10^{-3}$	$5.70 \times 10^{-3}$
	Mean	$1.62 \times 10^{-3}$	$3.79 \times 10^{-3}$	$5.085 \times 10^{-6}$	$1.50 \times 10^{-5}$	$1.63 \times 10^{-3}$	$3.80 \times 10^{-3}$	$1.63 \times 10^{-3}$	$3.80 \times 10^{-3}$	$1.63 \times 10^{-3}$	$3.80 \times 10^{-3}$
	SD	$4.81 \times 10^{-4}$	$1.12 \times 10^{-3}$	$1.51 \times 10^{-6}$	$4.45 \times 10^{-6}$	$4.83 \times 10^{-4}$	$1.13 \times 10^{-3}$	$4.83 \times 10^{-4}$	$1.13 \times 10^{-3}$	$4.83 \times 10^{-4}$	$1.13 \times 10^{-3}$
Average	1.70	3.96	5.37	1.59	2.24	5.55	$5.85 \times 10^{-4}$	$1.37 \times 10^{-3}$	$1.09 \times 10^{-4}$	$3.22 \times 10^{-4}$	

times greater for children than adults (Table 3), which is inconsistent with the results of Islam et al. (2020a) in six river basins in Bangladesh who found adults were more susceptible than children. For both age populations, it was found that Cd and Pb concentrations play a crucial role in triggering non-carcinogenic risk followed by Cr, whereas Zn contributes to less effect among HMs. Additionally, HMs followed the decreasing HQ values: Cd > Pb > Cr > Mn > Ni > Zn, respectively, for both age groups where Cd had the highest CDI value ( $5.58 \pm 5.11$  for adults and  $13.02 \pm 11.93$  for children) compared with other metals. HQ ingestion and dermal values of children were 2.33, and 2.93 times higher than that of the adult. In terms of HMs, Cd has the greatest health risk (Adult: 19.18; children: 44.75), especially in SW7, followed by Pb (Adults: 4.89; children: 11.42), especially in SW2. Thus, these two pollutants should first be controlled for public health safety and aquatic life.

Among these HMs, Cd, Cr and Pb have significant carcinogenic risks to the public health perspective. As shown in Table 3, the carcinogenic risk of Cd was comparatively higher in all sampling sites, which exceeded  $1 \times 10^{-4}$  for both age groups, indicating unacceptable carcinogenic risks, especially in children. The carcinogenic risk values of other metals (e.g., Pb, Cr) for both age groups were between  $1 \times 10^{-6}$  and  $1 \times 10^{-4}$ , except for some sites, indicating tolerable cancer risks. The outcomes of carcinogenic risk via the ingestion route of Cd were greater (adults:  $1.06 \times 10^{-3} \pm 9.71 \times 10^{-3}$ , children:  $2.47 \times 10^{-3} \pm 2.27 \times 10^{-3}$ ) than those for Pb (adults:  $4.11 \times 10^{-5} \pm 9.52 \times 10^{-6}$ , children:  $9.60 \times 10^{-5} \pm 2.22 \times 10^{-5}$ ) and Cr (adults:  $6.54 \times 10^{-4} \pm 1.80 \times 10^{-4}$ ; children:  $1.53 \times 10^{-3} \pm 4.19 \times 10^{-4}$ ). Generally, variations in the carcinogenic risk of Cd, Pb and Cr along the sampling sites are illustrated in Fig. 6. Also, sampling sites were followed the decreasing carcinogenic values: SW7>SW5>SW1>SW2>SW8>SW9>SW6>SW3>SW4. This is because SW7 is located near the dumping sludge side in the Dakovono creek and Cd and Pb emitted from goldmine and mineral processing activities may enter into the aquatic environment via atmospheric deposition, surface runoff, and eventually enriched in the surface water system. Nearly 90% and 95% of samples pose an elevated carcinogenic risk due to Cd amongst the age groups of the VGR of Fiji people, whereas the rest of the samples depict medium carcinogenic risk. Likewise, the carcinogenic risk via dermal values of

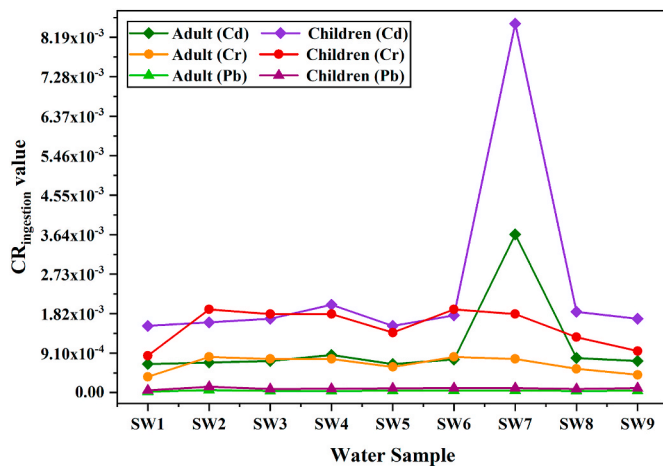


Fig. 6. Variations in carcinogenic risk of Cd, Cr and Pb for both adults and children through ingestion pathway in the surface water along the sampling sites.

Cd was followed by analogous patterns.

The outcome disclosed that the carcinogenic values of Cd were two folds of magnitude higher than that of Pb and Cr for adults and three and two folds of magnitude greater than those for children (Table S7). Besides, the carcinogenic ingestion risk values of Cd were also much greater than those of carcinogenic dermal values in the study region. The high intake of Cd disrupts the essential function of Ca and Zn in the living cell, therefore, in cellular metabolism (Ali et al., 2018). The outcomes demonstrate that Cd poses an unfavorable risk to the local wildlife and human health. Thus, continuous assessment in the VGR with high carcinogenic risk values is implied to avoid the accumulation

of Cd and other toxic metals such as Pb and Cr that could pose adverse health consequences, especially the policymakers should pay special attention to children due to the common surpassing  $1 \times 10^{-4}$ .

Monte-Carlo outcomes revealed that when quantile was considered, the CR value of Cd was significantly higher than  $1 \times 10^{-4}$ , even reaching  $2.55 \times 10^{-4}$  for children and reaching  $4.74 \times 10^{-5}$  for adults under the 90th quantile (Supplementary Table S8). The Cd values exceeded  $1 \times 10^{-4}$  and had evident carcinogenic risks for both populations. The mean carcinogenic risks of Cd were  $3.00 \times 10^{-5}$  and  $1.62 \times 10^{-4}$  for adults and children, respectively. The high Cd concentration may be due to gold mineral processing inputs, mostly of non-ferrous toxic metals. A recent study has also been reported that surface water in the vanadium-mining areas had the highest Cd pollution in Brazil (Santana et al., 2020). Ingestion exposure by drinking water of Cd might have a serious risk to both wild ecosystems and human health. Further, countermeasures should be needed for removal of Cd in the waters in the study area. In fact, Cd exists in water as a divalent cation ( $Cd^{2+}$ ) form with other elements (e.g.,  $CdCl_2$ ), which exhibits an elevated level of toxicity for humans and aquatic life (Bernhoft, 2013). Therefore, it is necessary to conduct an urgent epidemiological survey, should follow strict guidelines and continuous monitoring program concerning this elevated carcinogenic risk in the adjacent area of VGR.

### 3.5. Ecological risk assessment of HMs in sediment

Ecological indices such as  $I_{geo}$ , and PLI values for the selected six HMs in the sediments of the VGR are shown in Fig. 7. The pollution load index (PLI) values calculated from the six HMs ranged from 1.933 to 5.145 with an average value of 3.11. For appraising the sequential contamination status, PLI values for all sampling sites were computed and were plotted in Fig. 7a to understand the actual distributions of the integrated PHM's loads. All the PLI values are greater than unity in all

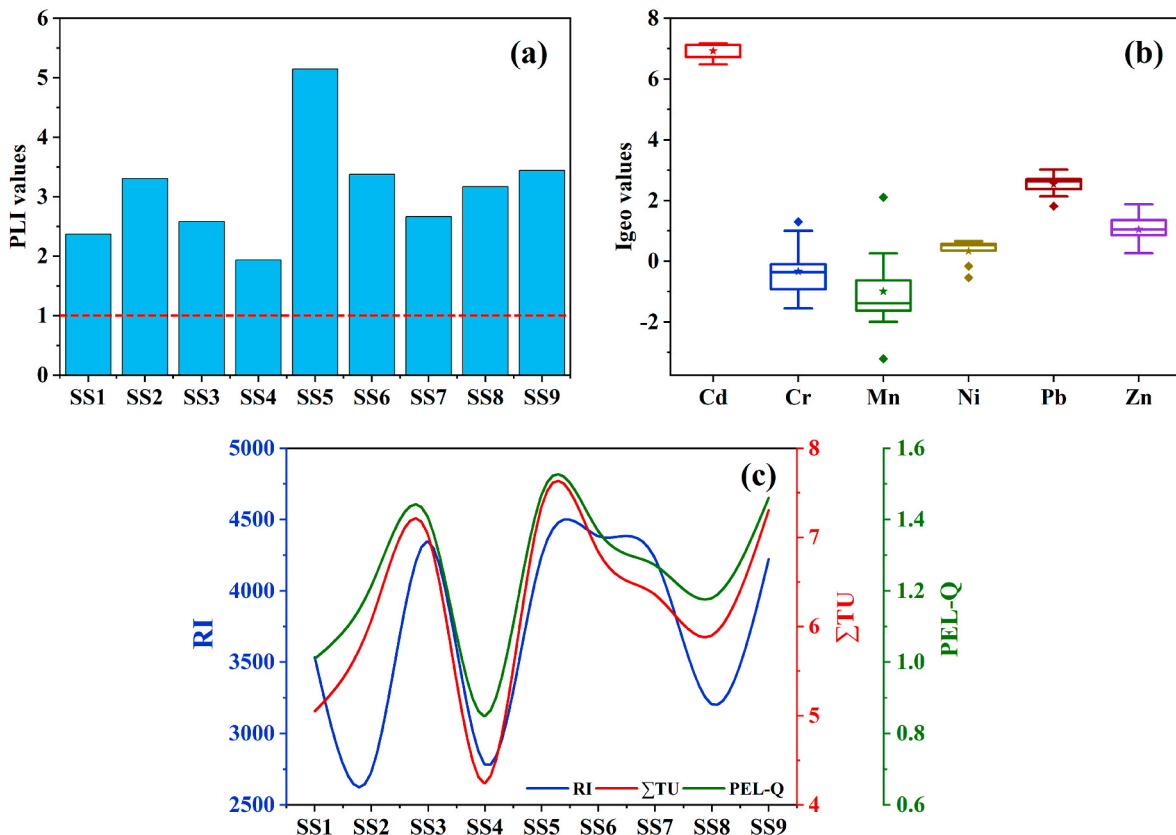


Fig. 7. Environmental and ecological indices for the sediment samples in the VGR. (a) Pollution load indices (PLI) for nine sampling sites in the study area; (b) Geo-accumulation index ( $I_{geo}$ , mean value of  $n = 9$ ); (c) values of  $\Sigma TU$ , PEL-Q and RI indices in the surface sediment samples.

sampling points. In the sampling sites SS-05, SS-02, SS-06, and SS-09, pollution loads are comparatively higher than other sampling points. However, SS-04 shows the lowest pollution load with time since the exploitation of mine activities.

$I_{geo}$  is a vital ecological index used to differentiate natural and human-induced sources of metals, and appraise the pollution level of sediment samples (Bastami et al., 2014). As seen in Fig. 7b, according to the average  $I_{geo}$  values, contamination of the HMs in the study area was demarcated in the order of  $Cd > Pb > Zn > Ni > Cr \gg Mn$ . The highest  $I_{geo}$  value was observed for Cd (6.923) in sites SS-05, whereas the lowest  $I_{geo}$  value was detected for Mn (−0.99) in site SS-04. The highest (at SS-05) and the lowest (at SS-04) contamination levels were observed in sampling sites located in the middle parts of the VGR. The  $I_{geo}$  classification of “extremely contaminated” was detected for Cd in the surface sediments from the sites SS-05; and “moderately to heavily contaminated” was identified for Pb and the “moderately contaminated” was detected for Zn in the sample site. Similar findings were reported by Song et al. (2019) in Zhaoyuan city goldmine, China. Compared with the background values (Table 2) in an earlier section, the Vatukoula Goldmine sediments are considered as contaminated with Cd, Pb, Zn and Ni, which exceeded the recommended levels at all sampling sites. In terms of  $I_{geo}$  values for most of the HMs, it suggests that the analyzed sites pose “moderately to extremely contaminated” status. Previous studies have stated that sediments, and tailing dams have a high accumulation of HMs around gold mining and processing areas (Souza et al., 2017; Huang et al., 2020), which is consistent with our study.

The sediment quality guideline values ( $\Sigma TU$  and PEL-Q), as well as the probable ecological risk, were appraised to confirm the analyses performed in this work. The sum of the toxic units ( $\Sigma TU$ ) showed the highest value (~7.35) in the sites SS5 and the lowest value in the sites SS4 (~4.24). The  $\Sigma TU$  and PEL-Q indices varied from 4.245 to 7.350 (mean value 6.236) and 0.849 to 1.470 (mean value 1.247), therefore suggesting that the coupling of the contaminants has a 75% possibility of toxic and triggering mortality of aquatic ecosystems, high species richness and liver lesions in several fish species (Long et al., 1995). For example, Cd concentrations were 3 times higher than the probable effect level (PEL) in the sediment sample from SS-05, indicating high phytotoxicity and potential bioaccumulation with likely harmful implications for both ecological and human health (Olafisoye et al., 2013). Surprisingly, the values for the studied HMs were more than 400; thus, they pose a very high potential ecological risk. The RI values varied from 2734.69 to 4344.83 with a mean value of 3742.23, which conforms to the results of Santana et al. (2020) in Vanadium mine, Brazil. All sampling sites exhibited values of  $RI > 400$ , suggesting a very high total likely ecological risk. However, in this study we did not report Cu, As, Sb, and Hg abundances in the sediment samples which toxicity response factors (T<sub>r</sub>: 5, 10, 10 and 40, respectively) are relatively higher (Khan et al., 2019; Islam et al., 2017). Thus, if the contributions of those chalcophile elements (Cu, As, Sb, and Hg) were considered, the RI will have even higher values.

The accumulated assessment of the  $\Sigma TU$ , PEL-Q, and RI indices permitted us to have a clear idea of the HM's contamination in the VGR (Fig. 7c). As can be seen, mining has a substantial effect on the surface sediment of this area. The maximum values for the three indices in SS-03, and SS-05 support that the goldmine is attributed to the elevated HMs in the study region. Likewise, the sampling sites SS-08 and SS-09 were 3 km far from goldmine that exhibited a smaller extent. These indices give an insight into the quality of the sediments and provide useful information to policymakers on the pollution level of aquatic ecosystems. Though high significant ecological risk was detected for all analyzed sites, it is crucial to shed light on the RI values (>2500) were found in the VGR that is alarming for all living organisms. If we considered that goldmine work in the VGR started in the past 80 years ago, that it extends for the next 10 years and that in the period an effect on the quality of these aquatic ecosystems is now apparent; the outcomes found in this work establish a quick “wake-up” call to perform

immediate actions to prevent and preserve these valuable surface sediments.

#### 4. Conclusion

This research gives an inclusive picture of the concentration status, level of contamination, source apportionment, co-existence, and associated ecological and human health risks from HM's exposures in water resources from the VGR, Fiji. Results show that the toxic metals in the study area are above guideline values and are highly polluted with them. The polluted water and sediment samples pose very high ecological and health risks. The principal component and positive matrix factorization analyses identified four potential pollution sources including i) gold mining inputs (Cd); ii) geogenic sources (Mn, and Ni); iii) gold mineral processing emission (Pb); iv) mixed effect of mining and geogenic sources (Cr and Zn). The findings revealed that geogenic processes intensified by goldmine activities may trigger elevated risks to aquatic lives and human health, particularly in children. Such information is important to recognize potentials for health sector developments and improve risk mitigation plans. The HMs research deserves attention in the Nasivi River because of the high concentrations indicating the high potential risk; especially all mining inputs come into this river, where these HMs are in direct contact with the local community.

Based on the research findings, it is found that the level of contamination and risks of HMs were high in water and sediment. Urgent attempts should be required to protect the Nasivi River from pollution and also to lessen environmental hazards. The outcomes obtained from this research highlight the necessity to plan and adopt efficient environmental management strategies and methods to reduce the contamination of HMs, particularly from the Toko tailing dam positioning nearby the urban sites, to diminish as much as potential human health risks for local inhabitants. For example, the tree plantation might be an alternative solution in the vicinity of the Toko tailing dam to decrease fast wind speed, in particular during the dry summertime matching with the plant growth stage, and hence limit the re-suspension of contaminated HMs in the surrounding environment. However, potentially toxic HMs e. g., Cu, As, Sb, Hg were not considered in this study which will certainly increase the ecological risk and probabilistic health risks estimation. Further study should attempt to conduct epidemiological research for severe pollution levels in the region. Regular monitoring of the pollution level, and the assessment of the impact on the environment and the local community, are strongly suggested to inform the people and the national and international organizations of the environmental risks associated with mining inputs; as well as to start an elaborate sustainable remediation policy that could be adopted to mitigate the contamination of freshwater resource by mining impurities. This study can certainly aid the management and policymakers take the necessary steps to lessen the impact of mining wastes on the aquatic environment and human health. Our work will also assist the environmental regulatory bodies and the mine managers to efficiently pollution control and the long-term effect of the mining activities on the soils and water resources around the mine area, and hence direct remediation and protection actions are needed. Although the study areas are chosen from Fiji, the outcomes have a broader policy direction for HMs contamination occurring from mining actions in other regions of the world.

#### Ethical approval

Not applicable.

#### Data availability

Data are available upon request on the corresponding author.

## Author contributions

S. K., and A.R.M.T.I., designed, planned, conceptualized, drafted the original manuscript, and H.M.T.I., and M.H., was involved in statistical analysis, interpretation; S.K., and R.K., contributed instrumental setup, data analysis, validation; V.O., contributed to editing the manuscript, literature review, proofreading; R.K., J.M., and A.R.M.T.I., were involved in software, mapping, and proofreading during the manuscript drafting stage.

## Declaration of competing interest

The authors declare that they have no known competing financial interests or personal relationships that could have appeared to influence the work reported in this paper.

## Acknowledgment

The authors are appreciative to their respective institutions of affiliation for the material support. A lot of thanks go to staffs in Chemistry Department at The University of the South Pacific for facilitating analysis of the samples. We acknowledge to Bangladesh Atomic energy Commission, Bangladesh for other kinds of experimental support during this work. The authors extend their appreciation to the Deanship of Scientific Research at King Khalid University for funding this work through Research Group under grant number (R.G.P.2/194/42).

## Appendix A. Supplementary data

Supplementary data to this article can be found online at <https://doi.org/10.1016/j.jenvman.2021.112868>.

## References

- Ackley, M., 2008. Evaluating Environmental Risks in Mining: a Perceptual Study at the Vatukoula Goldmine in Fiji. MSc Thesis. The University of Vermont, USA.
- Adeyemi, A.J., Laniyan, T.A., 2020. Contamination, sources and risk assessments of metals in media from Anka artisanal gold mining area, Northwest Nigeria. *Sci. Total Environ.* 137235.
- Ali, M.M., Ali, M.L., Islam, M.S., Rahman, M.Z., 2018. Assessment of toxic metals in water and sediment of Pasur River in Bangladesh. *Water Sci. Technol.* 77 (5), 1418–1430. <https://doi.org/10.2166/wst.2018.016>.
- Aldieri, L., Makkonen, T., Vinci, C.P., 2020. Environmental knowledge spillovers and productivity: a patent analysis for large international firms in the energy, water and land resources fields. *Resour. Pol.* 69, 101877.
- Amoakwah, E., Ahsan, S., Rahman, M.A., et al., 2020. Assessment of heavy metal pollution of soil-water-vegetative ecosystems associated with artisanal gold mining. *Soil Sediment Contam.: Int. J.* <https://doi.org/10.1080/15320383.2020.1777936>.
- Arikibe, J.E., Prasad, S., 2020. Determination and comparison of selected heavy metal concentrations in seawater and sediment samples in the coastal area of Suva, Fiji. *Mar. Pollut. Bull.* 157, 111157.
- Armah, F.A., Obiri, S., Yawson, D.O., Onumah, E.E., Yengoh, G.T., Afrifa Ernest, K.A., Odo, J.O., 2010. Anthropogenic sources and environmentally relevant concentrations of heavy metals in surface water of a mining district in Ghana: a multivariate statistical approach. *J. Environ. Sci. Health A* 45 (13), 1804–1813.
- Bastami, K.D., Bagheri, H., Kheirabadi, V., Zaferani, G.G., Teymori, M.B., Hamzehpoor, A., Soltani, F., Haghparast, S., Moussavi, H., Reza, S., Gorghani, N.F., Ganji, S., 2014. Distribution and ecological risk assessment of heavy metals in surface sediments along southeast coast of the Caspian Sea. *Mar. Pollut. Bull.* 81, 262–267.
- Bernhoft, R.A., 2013. Cadmium toxicity and treatment. *Sci. World J.* 1–7. <https://doi.org/10.1155/2013/394652>.
- BIS, 2012. Analysis of Water and Waste Water. Bureau of Indian Standards, New Delhi.
- Bodrud-Doza, M., Islam, A.R.M.T., Ahmed, F., Das, S., Saha, N., Rahman, M.S., 2016. Characterization of groundwater quality using water evaluation indices, multivariate statistics and geostatistics in central Bangladesh. *Water Sci.* 30, 19–40.
- Bokar, H., Traoré, A.Z., Mariko, A., Diallo, T., Traoré, A., Sy, A., Soumaré, O., Dolo, A., Bamba, F., Sacko, M., Touré, O., 2020. Geogenic influence and impact of mining activities on water soil and plants in surrounding areas of Morila Mine, Mali. *J. Geochem. Explor.* 209, 106429. <https://doi.org/10.1016/j.gexplo.2019.106429>.
- Brunner, A.M., Bertelkamp, C., Dingemans, M.M.L., et al., 2020. Integration of target analyses, non-target screening and effect-based monitoring to assess OMP related water quality changes in drinking water treatment. *Sci. Total Environ.* 705, 135779.
- Capparelli V., M., Moulattlet M., G., de Souza Abessa M., D., Lucas-Solis, O., Rosero, B., Galarza, E., Tuba, D., Carpintero, N., Ochoa-Herrera, V., Cipriani-Avila, I., 2020. An integrative approach to identify the impacts of multiple metal contamination sources on the Eastern Andean foothills of the Ecuadorian Amazonia. *Sci. Total Environ.* 709, 136088. <https://doi.org/10.1016/j.scitotenv.2019.136088>.
- Darwish, M.A.G., 2017. Reconnaissance geochemical survey in the Marahiq area, Wadi Allaqi region, south Egypt: a preliminary assessment of stream sediments for gold placer and environmental hazard. *Environ. Earth Sci.* 76 (23).
- Diarra, I., Prasad, S., 2020. The current state of heavy metal pollution in Pacific Island Countries: a review. *Appl. Spectrosc. Rev.* 1–23. <https://doi.org/10.1080/05704928.2020.1719130>, 0:0.
- EPA, 2005. Guidelines for Carcinogen Risk Assessment EPA/630/P-03/001F. Risk Assessment Forum. March 2005. U.S. Environmental Protection Agency, Washington, DC. Available: <http://cfpub.epa.gov/ncea/cfm/recordisplay.cfm?deid=116283>. (Accessed 10 September 2020).
- Fashola, M.O., Ngole-Jeme, V.M., Babalola, O.O., 2016. Heavy metal pollution from goldmines: environmental effects and bacterial strategies for resistance. *Int. J. Environ. Res. Publ. Health* 13, 1047.
- Fernandes, H.M., Franklin, M.R., Leoni, G.M., Almeida, M., 2004. A case study on the Uranium tailings dam of Pocos de Caldas uranium mining and milling site. *IAEA TECDOC*, p. 1403.
- Finkelmann, R.B., Orem, W.H., Plumlee, G.S., Selinus, O., 2018. Applications of geochemistry to medical geology. *Environ. Geochem.: Site Character. Data Anal. Case Hist.* 435–465.
- Florea, R.M., Stoica, A.I., Baiulescu, G.E., Capotă, P., 2005. Water pollution in gold mining industry: a case study in Roşia Montană district, Romania. *Environ. Geol.* 48 (8), 1132–1136. <https://doi.org/10.1007/s00254-005-0054-7>.
- FAO, 2003. The Irrigation Challenge: Increasing Irrigation Contribution to Food Security through Higher Water Productivity from Canal Irrigation Systems. IPTRID Is-sue Paper 4, IPTRID Secretariat, Food and Agricultural Organization of the United Nations, Rome.
- Gleeson, T., Wada, Y., Bierkens, M.F.P., van Beek, L.P.H., 2012. Water balance of global aquifers revealed by groundwater footprint. *Nature* 488, 197–200. <https://doi.org/10.1038/nature11295>.
- Habib, M.A., Islam, A.R.M.T., Bodrud-Doza, M., Mukta, F.A., Khan, R., Siddique, M.A.B., Phoungthong, K., Techato, K., 2020. Simultaneous appraisals of pathway and probable health risk associated with trace metals contamination in groundwater from Barapukuria coal basin, Bangladesh. *Chemosphere* 242, 125183.
- Hadzi, G.Y., Essumang, D.K., Ayoko, G.A., 2018. Assessment of contamination and health risk of heavy metals in selected water bodies around gold mining areas in Ghana. *Environ. Monit. Assess.* 190 (7).
- Hakanson, L., 1980. An ecological risk index for aquatic pollution control- A sedimentological approach. *Water Res.* 14 (8), 975–1001.
- Hemann, J.G., Brinkman, G.L., et al., 2009. Assessing positive matrix factorization model fit: a new method to estimate uncertainty and bias in factor contributions at the measurement time scale. *Atmos. Chem. Phys.* 9, 497–513.
- Huang, Y.N., Fei Dang, F., Li, M., et al., 2020. Environmental and human health risks from metal exposures nearby a Pb-Zn-Ag mine, China. *Sci. Total Environ.* 698, 134326.
- Islam, A.R.M.T., Ahmed, N., Bodrud-Doza, M., Chu, R., 2017. Characterizing groundwater quality ranks for drinking purposes in Sylhet district, Bangladesh, using entropy method, spatial autocorrelation index, and geostatistics. *Environ. Sci. Pollut. Res.* 24 (34), 26350–26374.
- Islam, A.R.M.T., Hasanuzzaman, M., Islam, H.M.T., et al., 2020a. Quantifying source apportionment, Co-occurrence and ecotoxicological risk of metals from up-mid-downstream river segments, Bangladesh. *Environ. Toxicol. Chem.* <https://doi.org/10.1002/etc.4814>.
- Islam, A.R.M.T., Islam, H.M.T., Mia, M.U., Khan, R., Habib, M.A., Bodrud-Doza, M., Siddique, M.A.B., Chu, R., 2020b. Co-distribution, possible origins, status and potential health risk of trace elements in surface water sources from six major river basin, Bangladesh. *Chemosphere* 249, 126180. <https://doi.org/10.1016/j.chemosphere.2020.126180>.
- Islam, A.R.M.T., Bodrud-doza, M., Rahman, M.S., Amin, S.B., Chu, R., Mamun, H.A., 2019. Sources of trace elements identification in drinking water of Rangpur district, Bangladesh and their potential health risk following multivariate techniques and Monte-Carlo simulation. *Groundwater Sustain. Develop.* 9, 100275.
- Islam, M.S., Ahmed, M.K., Raknuzzaman, M., Habibullah-Al-Mamun, M., Islam, M.K., 2015. Heavy metal pollution in surface water and sediment: a preliminary assessment of an urban river in a developing country. *Ecol. Indicat.* 48, 282–291.
- Jaishankar, M., Tseten, T., Anbalagan, N., Mathew, B.B., Beeregowda, K.N., 2014. Toxicity, mechanism and health effects of some heavy metals. *Interdiscipl. Toxicol.* 7 (2), 60–72.
- Jarup, L., 2003. Hazard of heavy metal contamination. *Br. Med. Bull.* 68, 167–182. <https://doi.org/10.1093/bmb/ldg032>.
- Jarvis, A.P., Younger, P.L., 2000. Broadening the scope of mine water environmental impact assessment: a UK perspective. *Environ. Impact Assess. Rev.* 20, 85–96.
- Kabir, M.M., Akter, S., Ahmed, F.T., Mohinuzzaman, M., Didar-ul-Alam, M., Mostofa, K. M.G., Islam, A.R.M.T., Niloy, N.M., 2021. Salinity-induced fluorescence dissolved organic matter influence co contamination, quality and risk to human health of tube well water in southeast coastal Bangladesh. *Chemosphere* 275, 130053.
- Kamunda, C., Mathuthu, M., Madhuku, M., 2018. Potential human risk of dissolved heavy metals in goldmine waters of Gauteng Province, South Africa. *J. Toxicol. Environ. Health Sci.* 10 (6), 56–63.
- Kapia, S., Rao, B.K.R., Sakulas, H., 2016. Assessment of heavy metal pollution risks in Yonki Reservoir environmental matrices affected by gold mining activity. *Environ. Monit. Assess.* 188 (10), 586. <https://doi.org/10.1007/s10661-016-5604-9>.
- Khan, R., Islam, H.M.T., Islam, A.R.M.T., 2021. Mechanism of elevated radioactivity in Teesta river basin from Bangladesh: radiochemical characterization, provenance and

- associated hazards. *Chemosphere* 264, 128459. <https://doi.org/10.1016/j.chemosphere.2020.128459>.
- Khan, R., Islam, M.S., Tareq, A.R.M., Naher, K., Islam, A.R.M.T., Habib, M.A., Siddique, M.A.B., Islam, M.A., Das, S., Rashid, M.B., Ullah, A.K.M.A., Miah, M.M.H., Masura, S.U., Bodrud-Doza, M., Sarker, M.R., Badruzzaman, A.B.M., 2020. Distribution, sources and ecological risk of trace elements and polycyclic aromatic hydrocarbons in sediments from a polluted urban river in central Bangladesh. *Environmental Nanotechnology. Monitor. Manag.* 14, 100318.
- Khan, R., Das, S., Kabir, S., Habib, M.A., Naher, K., Islam, M.A., Tamim, U., Rahman, A.K.M.R., Deb, A.K., Hossain, S.M., 2019. Evaluation of the elemental distribution in soil samples collected from ship-breaking areas and an adjacent island. *J. Environ. Chem. Eng.* 7.
- Kinimo, K.C., Yao, K.M., Marcotte, S., Kouassi, N.L.B., Trokourey, A., 2018. Distribution trends and ecological risks of arsenic and trace metals in wetland sediments around gold mining activities in central-southern and southeastern Côte d'Ivoire. *J. Geochem. Explor.* 190, 265–280.
- Kumar, S., Trivedi, P.K., 2016. Heavy metal stress signaling in plants. *Plant Metal Interact.* 585–603.
- Kusin, F.M., Awang, N.H.C., Hasan, S.N.M.S., Rahim, H.A.A., Azmin, N., Jusop, S., Kim, K.-W., 2019. Geo-ecological evaluation of mineral, major and trace elemental composition in waste rocks, soils and sediments of a gold mining area and potential associated risks. *Catena* 183, 104229.
- Lanocha-Arendarczyk, N., Kosik-Bogacka, D.I., Kalisinska, E., Sokolowski, S., Kolodziej, L., Budis, H., Safranow, K., Kot, K., Ciosek, Z., Tomska, N., Galant, K., 2016. Influence of environmental factors and relationships between vanadium, chromium, and calcium in human bone. *BioMed Res. Int.* 2016, 8340425.
- Li, Z.Y., Ma, Z.W., van der Kuijp, T.J., Yuan, Z.W., Huang, L., 2014. A review of soil heavy metal pollution from mines in China: pollution and health risk assessment. *Sci. Total Environ.* 468, 843–853.
- Long, E.R., MacDonald, D.D., Smith, S.L., Calder, F.D., 1995. Incidence of adverse biological effects within ranges of chemical concentrations in marine and estuarine sediments. *Environ. Manag.* 19, 81–97.
- Lymperopoulou, T., Tsakanika, L.-A., Ochsenkuehn-Petropoulou, M., 2017. Method validation for the determination of aqua regia extractable trace elements in soils. In: Poster Presented at the 10th International Conference on Instrumental Methods of Analysis: Modern Trends and Applications (IMA-2017), pp. 17–21. Heraklion-Crete, Greece. (Accessed 4 May 2020).
- Maata, M., Singh, S., 2008. Heavy metal pollution in Suva harbour sediments, Fiji. *Environ. Chem. Lett.* 6, 113–118. <https://doi.org/10.1007/s10311-007-0122-1>.
- MacDonald, D., Ingersoll, C.G., Berger, T.A., 2000. Development and evaluation of consensus-based sediment quality guidelines for freshwater ecosystems. *Arch. Environ. Contam. Toxicol.* 39 (1), 20–31.
- Matakarawa, S., 2018. Gold Mining and Acute Respiratory Infection in Children: A Retrospective Cohort Study in Vatukoula, Fiji. MSc Thesis. University of Canterbury, NZ.
- Mataki, M., Koshy, K.C., Lal, M., 2006. Baseline climatology of Viti Levu (Fiji) and current climatic trends. *Pac. Sci.* 60, 49–68.
- Mines, D.G., 2019. Dome goldmines. Retrieved from <https://www.domegoldmines.com.au/about-fiji/mining-in-fiji/>. (Accessed 29 November 2018).
- Mora, A., Jumbo-Flores, D., González-Merizalde, M., Bermeo-Flores, S.A., Alvarez-Figueroa, P., Mahlknecht, J., Hernández-Antonio, A., 2019. Heavy metal enrichment factors in fluvial sediments of an amazonian basin impacted by gold mining. *Bull. Environ. Contam. Toxicol.* <https://doi.org/10.1007/s00128-019-02545-w>.
- Morrison, R.J., Narayan, S.P., Gangaiya, P., 2001. Trace element studies in laucala bay, suva, Fiji. *Mar. Pollut. Bull.* 42, 397–404.
- MRD, 2005. Mineral Resources Department, Water Quality Guidelines for Toko Tailings Dam.
- Muller, G., 1979. Schwermetalle in den sedimenten des Rheins, Veränderungen Seit 1971. *Umschau* 79, 778–783.
- Ning, L., Liyuan, Y., Jirui, D., Xugui, P., 2011. Heavy metal pollution in surface water of linglong gold mining area, China. *Procedia Environ. Sci.* 10, 914–917. <https://doi.org/10.1016/j.proenv.2011.09.146>.
- Niane, B., Moritz, R., Guédron, S., Ngom, P.M., Pfeifer, H.R., Mall, I., Poté, J., 2014. Effect of recent artisanal small-scale gold mining on the contamination of surface river sediment: case of Gambia River, Kedougou region, southeastern Senegal. *J. Geochem. Explor.* 144, 517–527.
- Odukoya, A.M., Olobaniyi, S.B., Oluseyi, T.O., Adeyeye, U.A., 2017. Health risk associated with some toxic elements in surface water of Ilesha goldmine sites, southwest Nigeria. *Environmental Nanotechnology. Monitor. Manag.* 8, 290–296.
- Oduo, B.O., Nanos, N., Carbonell, G., Torrijos, M., Patel, J.P., Rodríguez Martín, J.A., 2018. Artisanal gold-mining in a rural environment: land degradation in Kenya. *Land Degrad. Dev.* <https://doi.org/10.1002/ldr.3078>.
- Olafisoye, O.B., Adefioye, T., Osibote, O.A., 2013. Heavy metals contamination of water, soil, and plants around an electronic waste dumpsite. *Pol. J. Environ. Stud.* 22, 1431–1439.
- Ongoma, V., Rahman, M.A., et al., 2021. Variability of diurnal temperature range over Pacific Island countries, a case study of Fiji. *Meteorol. Atmos. Phys.* 133, 85–95. <https://doi.org/10.1007/s00703-020-00743-4>.
- Palacios-Torres, Y., de la Rosa, J.D., Olivero-Verbel, J., 2020. Trace elements in sediments and fish from Atrato River: an ecosystem with legal rights impacted by gold mining at the Colombian Pacific. *Environ. Pollut.* 256, 113290.
- Pandey, L.K., Park, J., Son, D.H., Kim, W., Islam, M.S., Choi, S., Lee, H., Han, T., 2019. Assessment of metal contamination in water and sediments from major rivers in South Korea from 2008 to 2015. *Sci. Total Environ.* 651, 323–333.
- Pavilonis, B., Grassman, J., Johnson, G., Diaz, Y., Caravanos, J., 2017. Characterization and risk of exposure to elements from artisanal gold mining operations in the Bolivian Andes. *Environ. Res.* 154, 1–9.
- Pereira, W.V.D.S., Renato Alves Teixeira, R.A., de Souza, E.S., et al., 2020. Chemical fractionation and bioaccessibility of potentially toxic elements in area of artisanal gold mining in the Amazon. *J. Environ. Manag.* 267, 110644.
- Pratap, A., Mani, F.S., Prasad, S., 2020. Heavy metals contamination and risk assessment in sediments of Laucala Bay, Suva, Fiji. *Mar. Pollut. Bull.* 156, 111238. <https://doi.org/10.1016/j.marpolbul.2020.111238>.
- Rakotondrabe, F., NdamNgoupayou, J.R., Mfonka, Z., Rasolomanana, E.H., NyangonoAbolo, A.J., AkoAko, A., 2018. Water quality assessment in the Bétaré-Oya gold mining area (East-Cameroon): multivariate Statistical Analysis approach. *Sci. Total Environ.* 610–611, 831–844.
- Rudnick, R.L., Gao, S., 2014. Composition of the Continental Crust. *Treatise on Geochemistry*, second ed., p. 1e64 (Chapter 4).
- Santana, C.S., Montalván Olivares, D.M., Silva, V.H.C., Luzardo, F.H.M., Velasco, F.G., de Jesus, R.M., 2020. Assessment of water resources pollution associated with mining activity in a semi-arid region. *J. Environ. Manag.* 273, 111148.
- Santos, M.V.S., da Silva Júnior, J.B., et al., 2020. Geochemical evaluation of potentially toxic elements determined in surface sediment collected in an area under the influence of gold mining. *Mar. Pollut. Bull.* 158, 111384.
- Sako, A., Semdé, S., Wenmenga, U., 2018. Geochemical evaluation of soil, surface water and groundwater around the Tongon gold mining area, northern Côte d'Ivoire, West Africa. *J. Afr. Earth Sci.* <https://doi.org/10.1016/j.jafrearsci.2018.05.016>.
- Song, J., Liu, Q., Sheng, Y., 2019. Distribution and risk assessment of trace metals in riverine surface sediments in gold mining area. *Environ. Monit. Assess.* 191 (3).
- Souza, E.S., Texeira, R.A., da Costa, H.S.C., et al., 2017. Assessment of risk to human health from simultaneous exposure to multiple contaminants in an artisanal gold mine in Serra Pelada, Pará, Brazil. *Sci. Total Environ.* 576, 685–695.
- Tamim, U., Khan, R., Jolly, Y.N., Fatema, K., Das, S., Naher, K., et al., 2016. Elemental distribution of metals in urban river sediments near an industrial effluent source. *Chemosphere* 155, 509–518.
- Tchounwou, P.B., Yedjou, C.G., Patlolla, A.K., Sutton, D.J., 2012. Heavy metal toxicity and the environment. *Experientia Suppl.* 101, 133–164.
- Tomlinson, D.C., Wilson, J.G., Harris, C.R., Jeffrey, D.W., 1980. Problems in the assessment of heavy-metal levels in estuaries and the formation of a pollution index. *Helgol. Mar. Res.* 33, 566–575.
- US EPA, 2004. Risk Assessment Guidance for Superfund Volume 1. Human Health Evaluation Manual (Part E, Supplemental Guidance for Dermal Risk Assessment). U.S. Environmental Protection Agency. EPA/540/R/99/005 Office of Superfund Remediation and Technology Innovation, Washington, DC.
- USEPA, 2014. Environmental protection agency (EPA) positive matrix factorization (PMF) 5.0 fundamentals and user guide. US EPA, Off. Air Qual. Plan. Stand. Res. Triangle Park, NC.
- Ustaoglu, F., Islam, M.S., 2020. Potential toxic elements in sediment of some rivers at Giresun, Northeast Turkey: a preliminary assessment for ecotoxicological status and health risk. *Ecol. Indic.* 113, 106237.
- Varol, M., 2020. Environmental, ecological and health risks of trace metals in sediments of a large reservoir on the Euphrates River (Turkey). *Environ. Res.* 109664.
- Venkatraman, S., Chung, S.Y., Ramkumar, T., Selvam, S., 2015. Environmental monitoring and assessment of heavy metals in surface sediments at Coleroon River Estuary in Tamil Nadu, India. *Environ. Monit. Assess.* 187, 505.
- Vithanage, M., Kumarathilaka, P., Oze, C., Karunatilake, C., Seneviratne, M., Hseu, Z.Y., Gunarathne, V., Dassanayake, M., Ok, Y.S., Rinkbe, J., 2019. Occurrence and cycling of trace elements in ultramafic soils and their impacts on human health: a critical review. *Ecol. Indic.* 74, 182–190.
- Wang, H., Huang, J., Zhou, H., Deng, C., Fang, C., 2020. Analysis of sustainable utilization of water resources based on the improved water resources ecological footprint model: a case study of Hubei Province, China. *J. Environ. Manag.* 262, 110331.
- WHO, 2017. World Health Statistics 2017: Monitoring Health for the SDGs, Sustainable Development Goals. World Health Organization. <https://apps.who.int/iris/handle/10665/255336>.
- Xia, F., Zhang, C., Qu, L., Song, Q., Ji, X., Mei, K., Dahlgren, R.A., Zhang, M., 2020. A comprehensive analysis and source apportionment of metals in riverine sediments of a rural-urban watershed. *J. Hazard Mater.* 381, 121230.
- Xue, J.L., Zhi, Y.Y., Yang, L.P., Shi, J.C., Zeng, L.Z., Wu, L.S., 2014. Positive matrix factorization as source apportionment of soil lead and cadmium around a battery plant (Changxing County, China). *Environ. Sci. Pollut. Res.* 21, 7698–7707.
- Zanotti, C., Rotiroli, M., Fumagalli, L., et al., 2019. Groundwater and surface water quality characterization through positive matrix factorization combined with GIS approach. *Water Res.* 159, 122–134.
- Zhitkovich, A., 2011. Chromium in drinking water: sources, metabolism, and cancer risks. *Chem. Res. Toxicol.* 24 (10), 1617–1629. <https://doi.org/10.1021/tx200251t>.
- Zhang, H., Yu, J., Zhou, S., 2013. Spatial distribution of as, Cr, Pb, Cd, Cu, and Zn in the water and sediment of a river impacted by gold mining. *Mine Water Environ.* 33 (3), 206–216.
- Zhaoyong, Z., Abuduwaili, J., Fengqing, J., 2015. Heavy metal contamination, sources, and pollution assessment of surface water in the Tianshan Mountains of China. *Environ. Monit. Assess.* 187, 33.
- Zheng, N., Wang, Q., Liang, Z., Zheng, D., 2008. Characterization of heavy metal concentrations in the sediments of three freshwater rivers in Huludao City, Northeast China. *Environ. Pollut.* 154, 135–142.